The Ozonolysis of Acetylene—A Quantum Chemical Investigation

Dieter Cremer,*,† Ramon Crehuet,‡ and Josep Anglada*,‡

Contribution from the Department of Theoretical Chemistry, Göteborg University, Reutersgatan 2, S-41320 Göteborg, Sweden, and Departament de Quimica Organica Biologica, Institut d'Investigacions Quimiques i Ambientals de Barcelona, C.I.D.-CSIC, Jordi Girona 18, 08034-Barcelona, Catalunya, Spain

Received January 19, 2001

Abstract: The ozonolysis of acetylene was investigated using CCSD(T), CASPT2, and B3LYP-DFT in connection with a 6-311+G(2d,2p) basis set. The reaction is initiated by the formation of a van der Waals complex followed by a $[4\pi + 2\pi]$ cycloaddition between ozone and acetylene (activation enthalpy $\Delta H_a(298) = 9.6$ kcal/mol; experiment, 10.2 kcal/mol), yielding 1,2,3-trioxolene, which rapidly opens to α-ketocarbonyl oxide **5**. Alternatively, an O atom can be transferred from ozone to acetylene ($\Delta H_a(298) = 15.6$ kcal/mol), thus leading to formyl carbene, which can rearrange to oxirene or ketene. The key compound in the ozonolysis of acetylene is **5** because it is the starting point for the isomerization to the corresponding dioxirane **19** ($\Delta H_a(298) = 16.9$ kcal/mol), for the cyclization to trioxabicyclo[2.1.0]pentane **10** ($\Delta H_a(298) = 19.5$ kcal/mol), for the formation of hydroperoxy ketene **15** ($\Delta H_a(298) = 20.6$ kcal/mol), and for the rearrangement to dioxetanone **9** ($\Delta H_a(298) = 23.6$ kcal/mol). Compounds **19**, **10**, **15**, and **9** rearrange or decompose with barriers between 13 and 16 kcal/mol to yield as major products formanhydride, glyoxal, formaldehyde, formic acid, and (to a minor extent) glyoxylic acid. Hence, the ozonolysis of acetylene possesses a very complicated reaction mechanism that deserves intensive experimental studies.

1. Introduction

Although the ozonolysis of alkynes has been known for more than a century,[1] relatively little is known about the mechanism of this reaction.[2−14] This has to do with both the complexity of the reaction mechanism and the experimental difficulties in handling potentially explosive intermediates. Nevertheless, the reaction was and still is used in syntheses at reduced temperatures to determine the position of triple bonds of larger alkyne molecules,[15] to selectively oxidize the double bond in enyne molecules,[16] or to produce α-diketones and α-ketoesters from alkynes and acetylenic ethers.[1,17] Furthermore, the alkyne ozonolysis is known to produce epoxidization agents that are considerably stronger than peracids, but so far this has not been exploited in chemical synthesis because their structure and reactivity are unknown. Keay and Hamilton[6,7] provided evidence that similar epoxidation agents play a role in enzymatic reactions; however, final proof for the structure of these epoxidation agents is still missing.

There are several areas in chemistry for which the alkyne ozonolysis plays an important role and for which a better understanding of the reaction mechanism is desirable: (1) A more systematic use of the synthetic potential of the reaction requires detailed knowledge of its mechanism. (2) Wastewater and industrial sewage are often purified or treated with ozone,[18] and, in this connection, one has to know which compounds could be generated from alkynes. (3) The same applies to ozone−alkyne reactions in the polluted atmosphere. Actually, the alkyne ozonolysis is too slow to compete with OH radical−alkyne reactions;[19] however, the former can take place in the absence of OH radicals. (4) It is well-known that an increase of the ozone concentration in urban areas leads to the ozonolysis of terpenes emitted from bushes and trees.[19] Similarly, ozone can attack volatile natural products containing CC triple bonds and, by this, generate strongly epoxidizing agents in the atmosphere.

In recent work, we studied the ozonolysis of alkenes,[20−24] for which the Criegee mechanism is largely relevant.[25,26] There

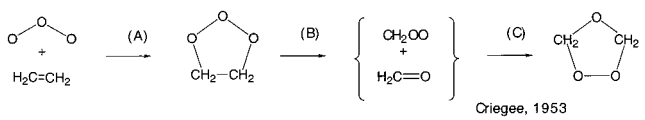

Criegee, 1953

has been a dispute for years over whether the Criegee mecha-

† Göteborg University.

‡ Institut d'Investigacions Quimiques i Ambientals de Barcelona, C.I.D.-CSIC.

(1) For a review, see: Bailey, P. S. In *Ozonation in Organic Chemistry, Volume II, Nonolefinic Compounds*; Academic Press: New York, 1982; Chapter 2.
(2) Criegee, R.; Lederer, M. *Liebigs Ann. Chem.* **1953**, *583*, 29.
(3) DeMore, W. B. *Int. J. Chem. Kinet.* **1969**, *1*, 209.
(4) DeMore, W. B. *Int. J. Chem. Kinet.* **1971**, *3*, 161.
(5) DeMore, W. B.; Lin, C. L. *Int. J. Org. Chem.* **1973**, *38*, 985.
(6) Keay, R. E.; Hamilton, G. A. *J. Am. Chem. Soc.* **1975**, *97*, 6876.
(7) Keay, R. E.; Hamilton, G. A. *J. Am. Chem. Soc.* **1976**, *98*, 6578.
(8) Jackson, S.; Hull, L. A. *J. Org. Chem.* **1976**, *41*, 3340.
(9) Pryor, W. A.; Govindan, C. K.; Church, D. F. *J. Am. Chem. Soc.* **1982**, *104*, 7563.
(10) Ando, W.; Miyazaki, H.; Ito, K.; Auchi, D. *Tetrahedron Lett.* **1982**, *23*, 555.
(11) Griesbaum, K.; Dong, Y.; McCullough, K. J. *J. Org. Chem.* **1997**, *62*, 6129.
(12) Griesbaum, K.; Dong, Y. *Liebigs Ann./Recl.* **1997**, 753.
(13) Griesbaum, K.; Dong, Y. *J. Prakt. Chem.* **1997**, *339*, 575.
(14) Dong Y.; Griesbaum, K.; Mccullough, K. J. *J. Chem. Soc., Perkin Trans. 1* **1997**, 1601.
(15) See, e.g.: Silbert, L. S.; Foglia, T. A. *Anal. Chem.* **1985**, *57*, 1404.
(16) McCurry, P. M., Jr.; Abe, K. *Tetrahedron Lett.* **1974**, 1387.
(17) Wisaksono, W. W.; Arens. J. F. *Recl. Trav. Chim. Pays-Bas* **1961**, *80*, 846.
(18) Bailey, P. S. In *Ozone in Water and Wastewater Treatment;* Evans, F. J., III, Ed.; Ann Arbor Sci. Publ.: Ann Arbor, MI, 1972; Chapter 3.
(19) (a) Finlayson-Pitts, B. J.; Pitts, J. N., Jr. *Atmospheric Chemistry: Fundamentals and Experimental Techniques*; Wiley: New York, 1986. See also: (b) Griesbaum, K.; Miclaus, V.; Jung, I. C. *Environ. Sci. Technol.* **1998**, *32*, 647.

10.1021/ja010166f CCC: $20.00
Published on Web 06/02/2001

Scheme 1

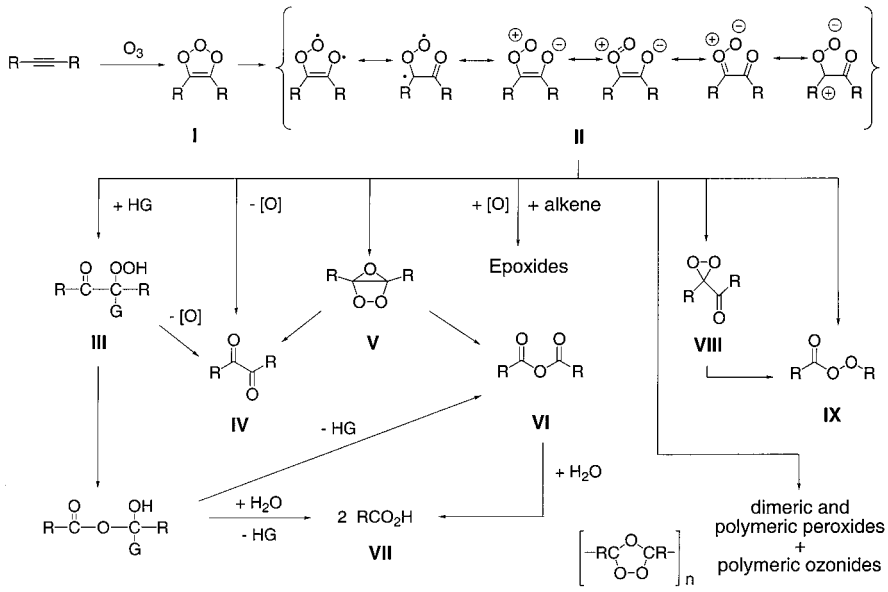

nism applies to both solution phases (where it has been verified) and the gas phase (where alternative mechanisms such as the O'Neil−Blumstein mechanism[27a] and other radical-driven mechanisms have been discussed[27b]). As we will show in this work, an investigation of alkyne ozonolysis is directly relevant for these questions since conclusions drawn for the ethene ozonolysis can be probed directly in the case of the ozone−acetylene reaction. Acetylene has two H atoms fewer than ethene, and, therefore, the ozonolysis mechanism of Criegee should become simpler. Also, it should be easier from a theoretical point of view to test alternatives to the Criegee mechanism which involve radicals or biradicals.

Hence, the aim of this work is threefold. First, we will use quantum chemical methods to elucidate the mechanism of the acetylene ozonolysis in detail and to draw general conclusions about the ozonation of alkynes. In this way, we want to improve the predictability of product distributions and, consequently, the applicability of the alkyne ozonolysis in synthesis. Second, we will establish the relevance of the acetylene ozonolysis for the mechanism of the alkene ozonolysis by comparing the two reactions, particularly with regard to their gas-phase and solution-phase mechanisms. Finally, we will suggest specific experiments that will lead to a confirmation of the results presented here and may also improve our understanding of labile oxidation intermediates in general.

We will proceed by first summarizing in section 2 what is known about the mechanism of the alkyne ozonolysis and what are the major questions and problems in this connection. Then, in section 3, we will lay the basis for an adequate quantum chemical description of the ozonolysis of acetylene. In section 4, we will present results on the reaction mechanism, which will be discussed in detail. Finally, in section 5, we will focus on the chemical relevance of calculational results.

2. Short Survey of Experimental Facts on the Alkyne Ozonolysis

In analogy to the Criegee mechanism of the ozonolysis of alkenes,[25,26] Criegee and Lederer[2] suggested in 1953 a concise mechanism for the alkyne ozonolysis, which focused on the formation of an α-keto carbonyl oxide **II** (also referred to as "vinylogous ozone",[7] see Scheme 1) via an ozone adduct **I**. Later work suggested that rearrangement of **II**, O-transfer reactions, or reactions with the solvent lead to a mixture (**III**−**IX**, Scheme 1) of carboxylic acids, anhydrides, α-diketones, dimeric (polymeric) peroxides, and ozonides as well as solvent adducts.[2−14] In protic solvents HG, α-keto hydroperoxides (**III**) are formed, thus verifying the existence of carbonyl oxide **II**. Often, compounds **III** are unstable and by reduction lead to α-diketone **IV**, which can also be formed directly from **II**. Recently, Griesbaum and Dong[12] developed a method to verify the intermediary of **III** and, thus, that of **II** by reaction with *O*-methyloximes and derivatization of **III** to the more stable α-iminohydroperoxides. In the absence of reducing agents in aprotic solvents, **II** rearranges, probably via the bicyclic ozonide **V**, to anhydride **VI**, which by solvolysis gives carboxylic acids **VII**. Ozonide **V** was suggested early;[1,8] however, experimental evidence for the existence of **V** was first given by Ando and co-workers.[10] Chemiluminescence was observed when **V** decomposed. Similar observations were made by Yang and Libman[28] and others[1,8] when ozone−alkyne reaction mixtures were warmed up. In methylene chloride, ozonides and other peroxidic compounds seem to represent 80% of the ozonation products, with diketone and carboxylic acids comprising the remainder.

While Criegee and Lederer[2] did not specify the nature of the ozone adduct, spectroscopic investigations by DeMore carried out for the acetylene ozonolysis in the gas phase verified the

(20) Cremer, D. *J. Am. Chem. Soc.* **1981**, *103*, 3619; *103*, 3627; *103*, 3633.

(21) (a) Gutbrod, R.; Schindler, R. N.; Kraka, E.; Cremer, D. *Chem. Phys. Lett.* **1996**, *252*, 221. (b) Gutbrod, R.; Kraka, E.; Schindler, R. N.; Cremer, D. *J. Am. Chem. Soc.* **1997**, *119*, 7330.

(22) Olzmann, M.; Kraka, E.; Cremer, D.; Gutbrod, R.; Andersson, S. *J. Phys. Chem.* **1998**, *101*, 99421.

(23) Cremer, D.; Kraka, E.; Olzmann, M., to be published.

(24) (a) Anglada, J. M.; Crehuet, R.; Bofill, J. M. *Chem. Eur. J.* **1999**, *5*, 1809. (b) Anglada, J. M.; Besalu, E.; Bofill, J. M.; Crehuet, R. *J. Comput. Chem.* **1999**, *20*, 1130.

(25) Criegee, R. *Liebigs Ann. Chem.* **1953**, *583*, 1.

(26) Bailey, P. S. *Ozonation in Organic Chemistry*; Academic Press: New York, 1978; Vol. I.

(27) (a) O'Neal, H. E.; Blumstein, C. *Int. J. Chem. Kinet.* **1973**, *5*, 397. (b) Bailey, P. S. *Ozonation in Organic Chemistry*; Academic Press: New York, 1978; Vol. I, p 232.

(28) Yang, N. C.; Libman, J. *J. Org. Chem.* **1974**, *39*, 1974.

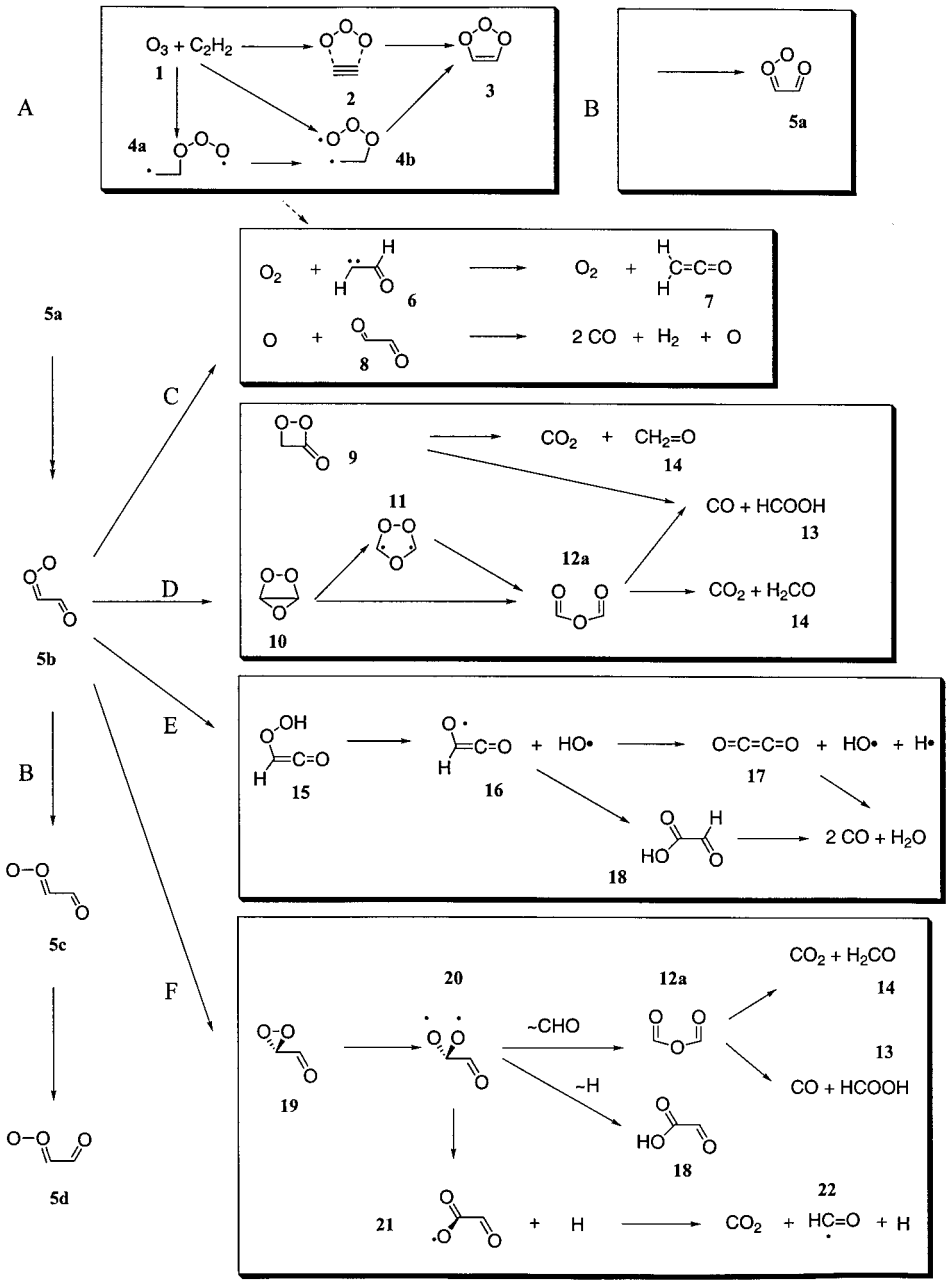

Figure 1. Mechanism of the ozonolysis of acetylene. The various steps of the reaction are called A (trioxolene formation), B (carbonyl oxide formation), C (oxygen loss), D (cyclization), E (OH production), and F (dioxirane formation).

formation of 1,2,3-trioxolenes **I**.[4,5] By a combination of microwave measurements and ab initio calculations, Gillies, Cremer, and co-workers[29] provided proof for the formation of **I** via a van der Waals complex. Colored van der Waals complexes were also found in the ozonation of methoxylated tolans (diphenylacetylenes) on silica gel.[30] Other intermediates of the alkyne ozonolysis have been discussed, and in this connection the work of Keay and Hamilton has to be mentioned.[6,7] These authors observed in the alkyne ozonolysis three different epoxidizing agents, X, Y, and Z, of which Z was identified to be peroxy acid. X and Y were stable at −70 to −50 °C and −50 to −15 °C and epoxidized in either a stereospecific (X) or a nonstereospecific manner (Y). As possible candidates for X and Y, trioxolene **I** and dioxirane **VIII** were considered.[6,7]

In the gas-phase ozonolysis of acetylene, CO, CO_2, formic acid, and glyoxal were detected.[4] On the basis of kinetic measurements, DeMore suggested a radical mechanism.[3] However, evidence for a free-radical pathway in the ozonolysis of dimethylacetylene was also found in the solution phase, where acetoxyl and acetyl radicals could be detected with suitable spin traps.[9] Apart from this, there is little evidence to determine whether the mechanism of the alkyne ozonolysis in the gas phase differs from that in solution phase and whether both mechanisms or just one of them proceeds predominantly via radical intermediates.[1]

Although the ozonolysis of alkynes should be mechanistically simpler than the ozonolysis of alkenes because of the smaller number of substituents at the CC multiple bond, all the experimental evidence suggests a complicated and hardly

(29) Gillies, J. Z.; Gillies, C. W.; Lovas, F. J.; Matsumura, K.; Suenram, R. D.; Kraka, E.; Cremer, D. *J. Am. Chem. Soc.* **1991**, *113*, 6408.

(30) (a) Laurent-Bouas, H.; Desvergne, J. P.; Lapouyade, R.; Thomas, J. M. *Mol. Cryst. Liq. Cryst.* **1976**, *32*, 143. (b) Desvergne, J. P.; Bouas-Laurent, H. *J. Catal.* **1977**, *51*, 126.

Table 1. Schematic Description of the Active Spaces Used in the CASSCF Calculations

species	space[a]	description
O_3	(6,6)	the bonding σ (b_2) and two π (b_1 and a_2) orbitals plus the two antibonding σ^* (a_1 and b_2) and π^* (b_1) orbitals
C_2H_2	(4,4)	the two π orbitals and the corresponding π^* orbitals
10	(10,10)	the four σ(CO), the σ (OO) and the corresponding antibonding orbitals
TS10-12a, 12c	(8,8)	the two $\sigma(CO_{terminal})$, the two $\pi(CO_{terminal})$, and the corresponding antibonding orbitals
11a, 11b TS10-11b	(8,8)	the two $\sigma(CO_{ether})$, the σ(OO), and the corresponding antibondings plus the two p orbitals on C describing the biradical structure
19b, 20 TS19b-20	(10,10)	the two σ(CO), the σ(OO), the $\sigma(CO_{carbonyl})$, the $\pi(CO_{carbonyl})$, and the corresponding antibonding orbitals
18	(6,6)	the $\sigma(CO_{carbonyl})$, the two π(CO), and the corresponding antibonding orbitals
TS20-18	(10,10)	the $\sigma(CO_{carbonyl})$, the $\pi(CO_{carbonyl})$, the $\pi(CO_{acid})$, and the corresponding antibonding orbitals, plus the two bonding and antibonding orbitals describing the H migration
TS20-12a	(10,10)	the π(OCO), the two σ(CO), the $\pi(CO_{carbonyl})$, the two σ^*(CO), the $\pi^*(CO_{carbonyl})$, the σ^*(CC), plus the two p orbitals on O describing the biradical structure, one of which is combined with the σ(CC) orbital
TS20-21	(8,8)	the σ(CO), the $\pi(CO_{carbonyl})$, the σ(CH), and the corresponding antibonding orbitals plus the two π orbitals on O describing the biradical structure

[a] (x,x) denotes the number of active electrons and the number of active orbitals.

understood reaction mechanism, with probably major differences between gas and solution phases and a strong dependence on the presence (absence) of protic solvents, reduction agents, or other reaction partners. Thus, one cannot speak of a Criegee or any other ozonolysis mechanism that is generally applicable in the case of alkynes. Many questions are unanswered:

(1) Which are the major epoxidation agents in the ozonolysis of alkynes? Which epoxidation agent is stable at what temperature? How can one use their O-transfer capacity in a synthetically useful way? (2) What role does the trioxolene **I** play in the alkyne ozonolysis? Can it also function as an epoxidation agent? Is its lifetime long enough for this purpose? (3) What is the electronic and energetic nature of α-keto carbonyl oxides? Can they be stabilized and experimentally investigated? (4) Is there a bicyclic ozonide **V**? What are its properties? Can it function as another epoxidation agent? (5) Is there a possibility of OH radical formation in the alkyne ozonolysis, similar to that recently discussed for the alkene ozonolysis?[21] (6) What role do dioxiranes **VIII** play in the alkyne ozonolysis? Do they also function as epoxidation agents, or do they decompose via bisoxy biradicals in a manner similar to that found for the parent dioxirane?[31,32] (7) How, exactly, are the α-diketones, anhydrides, and peracids formed? How are CO and CO_2 generated? (8) What radicals are involved? How are they formed? Is there any difference between gas-phase and solution-phase ozonolysis?

To answer these and other questions, we carried out a thorough quantum chemical investigation of the acetylene ozonolysis. On the basis of our results (see section 4), we partitioned the ozonation of acetylene into six mechanistic steps (see Figure 1), namely (A) the formation of the ozone primary adduct, (B) the formation of α-keto carbonyl oxide, (C) the loss of oxygen in the carbonyl oxide, (D) the cyclization of α-keto carbonyl oxide to four- or five-membered rings, (E) H migration in α-keto carbonyl oxide and OH production, and (F) isomerization of α-keto carbonyl oxide to the corresponding dioxirane and follow-up reactions. Each of these steps is investigated by calculating with various methods more than 60 different molecular structures and transition states. Actually, the product manifold of the acetylene ozonolysis will be even larger if one considers the various epoxidation possibilities and adducts with a particular solvent. Since considering these reactions would significantly extend the present work, we will present the epoxidation of alkenes by intermediates of the alkyne ozonolysis in a separate paper.[33] There, we will also focus on recent suggestions and extensions of the Criegee−Lederer mechanism published by Griesbaum and Dong.[13] In this way, we want to contribute to the solution of a chemical problem, which is difficult to solve experimentally since experimental chemistry seems to reach some of its limits in the alkyne ozonolysis.

3. Computational Methods

As shown in Figure 1, molecules **1**−**22**, a similarly large number of transition states (TSs), and suitable reference compounds such as OH, CO, CO_2, H_2O, O_2, etc. were investigated in this work. Many of the structures shown in Figure 1 possess unusual electronic features (radicals, biradicals, strained rings, carbenes, etc.) that require advanced ab initio methods covering, besides dynamic, also static electron correlation effects. Energies and geometries were calculated in these cases with the CASSCF method[34] employing analytical gradients.[35−37] The active space of a given structure was selected according to the fractional occupation of the natural orbitals (NOs)[38] generated from the first-order density matrix of a MRD-CI[39−41] wave function, which was based on the correlation of all valence electrons. The details of the active space chosen for the various reactions are collected in Table 1. In a preliminary step, CASSCF geometry optimizations and the characterization of the stationary points as minima or saddle points were carried out using the 6-31G(d,p) basis set.[42] In a second step, all CASSCF geometries were reoptimized using the more flexible 6-311+G-(2d,2p) basis set.[43] In a third step, the effects of dynamic valence-electron correlation on CASSCF energy differences were covered by performing CASPT2[44] single-point calculations.

In addition to the CASSCF and CASPT2 method, we used density functional theory (DFT)[45] extensively in connection with the empirically

(31) Cremer, D.; Kraka, E.; Szalay, P. G. *Chem. Phys. Lett.* **1998**, *292*, 97.
(32) Anglada, J. M.; Bofill, J M.; Olivella, S.; Sol, A. *J. Am. Chem. Soc.* **1996**, *118*, 4636.
(33) Kraka, E.; Anglada J. M.; Cremer, D., to be published.
(34) Roos, B. O. *Adv. Chem. Phys.* **1987**, *69*, 399.
(35) Baker, J. *J. Comput. Chem* **1986**, *7*, 385.
(36) Baker, J. *J. Comput. Chem* **1987**, *8*, 563.
(37) Bofill, J. M. *J. Comput. Chem.* **1994**, *15*, 1.
(38) Anglada, J. M.; Bofill, J. M. *Chem. Phys. Lett.* **1995**, *243*, 151.
(39) Buenker, R. J.; Peyerimhoff, S. D. *Theor. Chim. Acta* **1975**, *39*, 217.
(40) Buenker R. J.; Peyerimhoff, S. D. In *New Horizons of Quantum Chemistry*; Lowdin, P. O., Pullman, B., Eds.; Reidel: Dordrecht, The Netherlands 1983; Vol. 35, p 183.
(41) Buenker, R. J.; Philips, R. A. *J. Mol. Struct. (THEOCHEM)* **1985**, *123*, 291.
(42) Hariharan, P. C.; Pople, P. C. *Theor. Chim. Acta* **1973**, *28*, 213.
(43) (a) Krishnan, R.; Binkley, J. S.; Seeger, R.; Pople, J. A. *J. Chem. Phys.* **1980**, *72*, 650. (b) Krishnan, R.; Frisch, M.; Pople, J. A. *Chem. Phys.* **1980**, *72*, 4244.
(44) Anderson, K.; Malmqvist, P. A.; Roos, B. O. *J. Chem. Phys.* **1992**, *96*, 1218.
(45) (a) Kohn, W.; Sham, L. J. *Phys. Rev.* **1965**, *140*, A1133. (b) For a review, see: Parr, R. G.; Yang, W. *Density-Functional Theory of Atoms and Molecules*; International Series of Monographs on Chemistry 16; Oxford University Press: New York, 1989.

Table 2. Energies, Enthalpies, Entropies, and Dipole Moments of Structures **1**−**22** Located at the Acetylene−Ozone ($C_2O_3H_2$) PES As Calculated with Different Methods and the 6-311+G(2d,2p) Basis Set[a]

line no.	system	symmetry	method	ref	ΔE	$\Delta\Delta H(298)$	S	$\Delta G(298)$	μ	$\Delta H_f^0(298)$	comment
				Part A							
1a	**1**		RDFT		0	0	105.0	0	0.68	88.5*	exp ref[b]
1b			CCSD(T)		0	0	104.6	0	0.56		*b*
1c			CASPT2		0	0	105.5	0	0.53		
2a	**2**	C_s	RDFT	1a	−0.7	0.2	86.5	7.1	0.58		BSSE corr[b]
2b			CCSD(T)	1b	−1.1	−0.2	86.5	5.2	0.56	88.3	BSSE corr[b]
3a	**TS2-3**	C_s	RDFT	2	4.5	3.9	70.7	8.6	2.04		*b*
3b			CCSD(T)	2	10.2	9.6	70.7	14.4	1.85	97.9	*b*
4a	**3**	C_s	RDFT	1a	−65.1	−62.1	68.0	−51.1	2.93		*b*
4b			CCSD(T)	1b	−59.6	−58.0	67.7	−45.7	2.90	30.5	*b*
				Part B							
5	**TS3-5a**	C_1	RDFT	4a	5.3	4.3	66.4	4.8	3.13	34.8	
6	**5a**	C_s	RDFT	4a	−27.2	−27.0	71.0	−27.9	4.84	3.5	
7	**TS5a-5b**	C_1	RDFT	6	3.6	2.7	69.3	3.2	4.96	6.2	
8	**5b**	C_s	RDFT	6	−5.4	−5.3	71.1	−5.4	1.67	−1.8	
9	**TS5b-5c** (^1A)	C_1	UDFT	8	19.4	17.5	70.3	17.7	1.14	15.7	
10	**5c**	C_s	RDFT	8	−2.5	−2.5	70.8	−2.4	1.18	−4.3	
11	**TS5c-5d**	C_1	RDFT	8	8.9	7.9	69.6	8.3	4.01	6.0	
12	**5d**	C_s	RDFT	8	1.3	1.3	71.0	1.3	3.97	−0.6	
				Part C							
13	**TS1-6** (^1A)	C_1	CASPT2	1c	16.2	15.6	75.7	24.5	2.75	104.1	*b*
14	**6** ($^3A''$) + O_2 ($^3\Sigma_g^-$)	C_1	UDFT	8	56.2	52.9	110.9	41.0	2.02	51.1	
15	**6** (^1A) + O_2 ($^1\Delta_g$)	C_1	R/ROSS-DFT	8	92.3	88.8	107.0	78.1		87.0	$\Delta(S-T) = 6.3$
16	**TS6-7** (^3A) + O_2 ($^3\Sigma_g^-$)	C_1	UDFT	14	43.0	39.2	110.8	39.3	2.29	90.3	
17	**7** ($^3A''$) + O_2 ($^3\Sigma_g^-$)	C_1	UDFT	14	−20.3	−20.1	111.3	−20.3	2.80	31.0	
18	**7** + O_2 ($^1\Delta_g$)	C_{2v}	R/ROSS-DFT	8	13.9	11.5	104.6	1.5	1.53	9.7	exp 8.3
19	**8** (^1A_g) + O (^1D)	C_{2h}	R/UDFT	8	54.6	53.0	99.0	42.7	0	51.2	exp 54.2[c]
20	**8** (^3A_u) + O (^3P)	C_{2h}	UDFT	8	54.9	52.0	102.3	42.6	0	50.2	
21	**TS8**-CO (^1A) + O (^1D)	C_2	R/UDFT	19	63.8	57.2	102.6	56.1	0.66	108.4	*c*
22	2CO + H_2 + O (^1D)		R/UDFT	19	10.3	2.8	159.9	−15.4		54.0	exp 52.1[c]
				Part D							
23	**TS5b-9**	C_s	RDFT	8	26.2	23.6	67.0	24.8	4.08	21.8	
24	**9**	C_s	RDFT	8	−40.9	−40.0	67.5	−38.9	3.01	−41.8	
25	**TS9-14**	C_s	RDFT	24	27.9	25.8	69.4	25.2	3.10	−16.0	
26	**14** + CO_2	C_s	RDFT	24	−78.7	−80.4	103.4	−91.1	2.44	−122.2	exp −121.8
27	**Ts5b-10**	C_1	RDFT	8	20.4	19.5	66.6	20.8	3.39	17.7	
28a	**10**	C_s	RDFT	8	8.5	8.8	65.3	10.5	2.90	7.0	
28b			CASPT2	1c	−80.8	−77.0	65.4	−65.0	3.18	11.5	24a used
29	**TS10-11b**	C_1	CASPT2	28b	35.1	33.9	65.3	33.9	1.28	40.9	(10,10) space
30	**11a** (^1A)	C_2	CASPT2	28b	16.8	16.7	64.9	16.9	1.57	23.7	(10,10) space
31	**11b** (^1A)	C_1	CASPT2	28b	22.2	22.1	66.7	21.7	1.78	29.1	(10,10) space
32a	**TS10-12a**	C_s	UDFT	28a	14.7	12.7	65.8	12.5	2.99	19.7	
32b			CASPT2	28b	13.7	12.7	65.3	12.7	3.17	24.2	
33	**12a** (^1A)	C_2	RDFT	28a	−118.1	−117.3	71.5	−119.2	3.28	−110.3	
34	**12b** (^1A)	C_1	RDFT	28a	−118.3	−117.5	69.9	−118.9	3.43	−110.5	
35	**12c** ($^1A'$)	C_s	RDFT	28a	−121.1	−120.2	71.8	−122.1	1.82	−113.2	
36	**12a** (^3A)	C_1	UDFT	33	81.2	79.6	71.8	79.5	2.83	−30.7	
37	**TS12c-13** ($^1A'$)	C_s	RDFT	35	29.6	26.2	70.6	26.6	0.45	−87.0	
38	**13** + CO		RDFT	35	−0.4	−2.0	106.6	−12.3	1.53	−115.2	exp −117.0
39	**TS12c-14**	C_1	RDFT	35	51.3	47.9	69.8	48.5	3.30	−65.3	
40	**14** + CO_2		RDFT	35	−6.9	−9.0	103.4	−18.4	2.44	−122.2	exp −121.8
41	**14** ($^3A''$) + CO_2	C_s	U/RDFT	40	67.6	65.6	107.6	64.3	1.51	−56.6	
				Part E							
42	**TS5b-15**	C_1	RDFT	8	23.8	20.6	68.4	21.4	2.40	18.8	
43	**15**	C_1	RDFT	8	−21.5	−21.7	75.3	−22.9	1.70	−23.5	
44	**TS15-16**	C_1	RDFT	43	14.9	13.1	72.7	13.8	3.09	−10.4	
45	**16** ($^2A''$) + OH ($^2\Pi$)	C_s	UDFT	43	10.4	7.3	110.0	−3.1	2.63	−16.2	
46	**17**($^3\Sigma_g^-$) + H (^2S) + OH ($^2\Pi$)	$D_{\infty h}$	UDFT	45	72.7	67.4	133.9	60.3	0	51.2	
47	**18**	C_s	RDFT	43	−90.2	−88.6	69.9	−87.0	1.92	−112.1	
48	**TS18**-CO	C_1	RDFT	47	69.9	65.0	119.7	63.6	1.77	−47.1	
49	2CO + H_2O		RDFT	47	10.7	6.1	139.6	−14.7		−106.0	exp −110.6
				Part F							
50	**TS5a-19a**	C_1	RDFT	6	20.7	19.3	71.0	19.3	4.22	22.8	
51	**19a**	C_1	RDFT	6	−20.3	−20.1	71.9	−20.4	3.25	−16.6	
52	**TS5b-19b**	C_1	RDFT	8	18.1	16.9	69.8	17.3	2.15	15.1	
53	**TS5c-19b**	C_1	RDFT	10	24.5	23.2	70.4	23.3	2.12	18.9	
54	**19b**	C_s	RDFT	8	−19.9	−19.7	70.7	−19.6	0.28	−21.5	
55	**TS19b-20** (^1A)	C_1	CASPT2	54	23.3	21.8	70.2	21.8	0.31	0.3	(10,10) space
56	**20** ($^1A'$)	C_s	CASPT2	54	14.6	13.5	72.5	12.9	0.35	−8.0	(10,10) space
57	**TS20-12a** (^1A)	C_1	CASSCF	56	2.8	2.1	70.2	2.8	0.16	−5.9	(10,10) space

Table 2. (Contd.)

line no.	system	symmetry	method	ref	ΔE	$\Delta\Delta H(298)$	S	$\Delta G(298)$	μ	$\Delta H_f^0(298)$	comment
58	**TS20-18** (^1A)	C_1	CASSCF	56	8.5	6.3	70.8	6.8	2.22	−1.7	(10,10) space
59	**TS20-21** (^1A)	C_1	CASPT2	56	23.2	18.3	71.8	18.5	2.49	10.3	(10,10) space
60	**21** ($^2A'$) + H (^2S)	C_s	UDFT	54	24.8	18.4	99.9	9.7	2.15	3.4	
61	**TS21-22** + H (^2S)		UDFT	60	1.1	−0.2	99.8	−0.2	2.33	3.2	
62	**22** ($^2A'$) + CO_2 + H (^2S)	C_s	UDFT	60	−31.2	−32.9	132.2	−42.5	1.68	−29.5	

[a] For a definition of structures, see Figure 1. Relative energies ΔE, zero-point energies ZPE, enthalpy differences $\Delta H(298)$, and free enthalpy differences $\Delta G(298)$ in kcal/mol, dipole moment μ in Debye, entropies S in cal mol/deg. − Each calculation has a number, which is given in the first column and used to define for a particular system the reference (column ref.) with regard to which energy and enthalpy differences are given. − The symmetry in column *Sym.* is given with regard to the first molecule in a system of two or more molecules; the same holds for the dipole moment. − ZPE and *S* values as well as temperature coprrections were calculated with the 6-31G(d,p) basis set if not indicated otherwise (see last column). In the case of CASPT2/6-311+G(2d,2p) and CASSCF/6-311+G(2d,2p) calculations, the vibrational corrections were determined at CASSCF/6-31G(d,p). − For each state, the most reliable energy obtained was used to calculate $\Delta H_f^0(298)$ values. The experimental heat of formation used as reference is indicated by a star. [b] ZPE, S, and temperature corrections calculated at B3LYP/6-311+G(2d,2p). CCSD(T)/6-311+G(2d,2p) geometry optimizations. [c] O(^3P) was calculated and the experimental energy difference of 45.4 kcal/mol added to obtain the energy of the O(^1D) state.

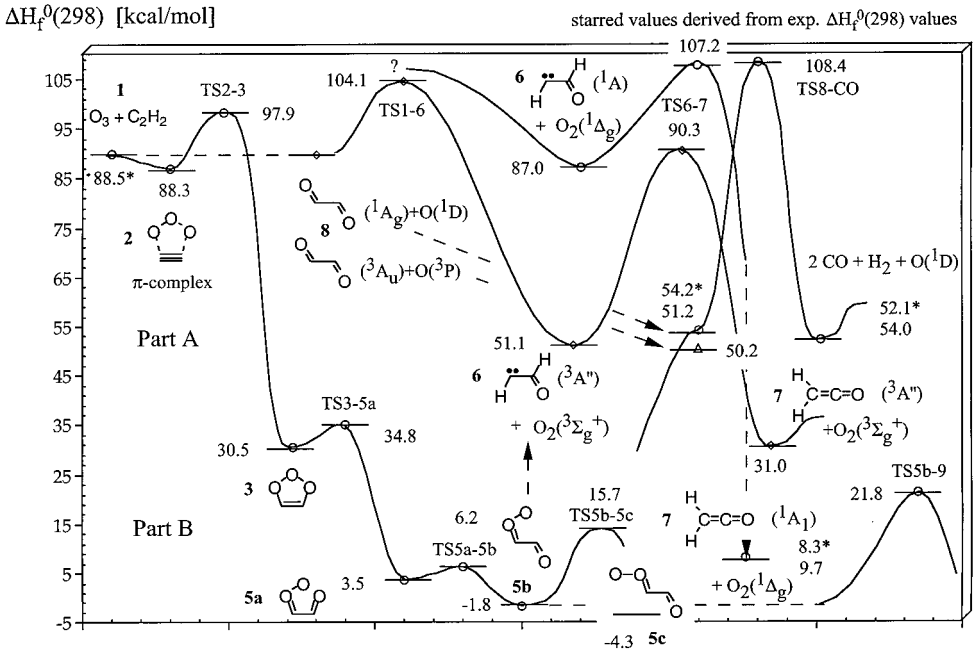

Figure 2. Energy diagram of steps A, B, and C of the acetylene ozonolysis (compare with Figure 1). Calculated heats of formation $\Delta H_f^0(298)$ (in kcal/mol) are given for each structure. Experimental $\Delta H_f^0(298)$ values are indicated with asterisks.

parametrized B3LYP hybrid functional.[46] Cremer and co-workers[21,31] showed that the B3LYP description of carbonyl oxide is similar to that obtained with CCSD(T). The energetics of the ozonolysis of ethylene calculated at the B3LYP level compare well with those obtained at the CCSD(T) level.[22] In recent work, it was also shown that UDFT is able to describe singlet biradicals satisfactorily in many cases.[47] Therefore, both restricted and unrestricted DFT (RDFT and UDFT) theory was applied to describe the reactions shown in Figure 1, where UDFT was used for radicals, singlet biradicals, and also the closed-shell systems, which turned out to be unstable at the RDFT level of theory.[48] For some biradicals, two-determinantal DFT was applied using the restricted open-shell singlet (ROSS) method of Gräfenstein, Kraka, and Cremer.[49] At all DFT levels of theory, geometry optimizations with the 6-31G(d,p) basis set and the more reliable 6-311+G(2d,2p) basis set were carried out. DFT energies and geometries of molecules with multireference character were compared with CASSCF and CASPT2 results to verify their reliability.

In the case of the formation of 1,2,3-trioxolene (**3**, Figure 1A), it turned out that neither CASPT2 nor DFT provided reliable results for the [4 + 2] cycloaddition reaction; therefore, geometry optimizations were repeated with the more reliable CCSD(T) method[50] and the 6-311+G(2d,2p) basis set. Since the formation of **3** implies that van der Waals complex **2** is a precursor (Figure 1), it was necessary to correct for basis set superposition errors (BSSEs) by utilizing the counterpoise method of Boys and Bernardi.[51]

In many cases, it had to be clarified to what reactant or product a given TS was connected by a reaction path. This was done by performing intrinsic reaction coordinate (IRC) calculations at the CASSCF or DFT level of theory.[52] Starting at a given TS, the reaction path, described in mass-weighted coordinates, was followed in the forward and backward directions until the reactant, the TS, and the product connected by the path could be clearly identified.

All stationary points found on the acetylene−ozone potential energy surface (PES) were characterized with the help of harmonic vibrational

(46) (a) Becke, A. D. *J. Chem. Phys.* **1993**, *98*, 5648. See also: (b) Stevens, P. J.; Devlin, F. J.; Chablowski, C. F.; Frisch, M. *J. Phys. Chem.* **1994**, *98*, 11623. (c) Becke A. D. *Phys. Rev. A* **1988**, *38*, 3098. See also: (d) Lee, C.; Yang, W.; Parr, R. G *Phys. Rev. B* **1988**, *37*, 785.

(47) (a) Gräfenstein, J.; Hjerpe, A. M.; Kraka, E.; Cremer, D. *J. Phys. Chem. A* **2000**, *104*, 1748. (b) Gräfenstein, J.; Kraka, E.; Filatov, M.; Cremer, D. *J. Phys. Chem. A*, submitted. See also: (c) Perdew, J. P.; Savin, A.; Burke, K. *Phys. Rev. A* **1995**, 51, 4531.

(48) Bauernschmitt, R.; Ahlrichs, R. *J. Chem. Phys.* **1996**, *104*, 9047.

(49) Gräfenstein, J.; Kraka, E.; Cremer, D. *Chem. Phys. Lett.* **1998**, *288* 593.

(50) Raghavachari, K.; Trucks, G. W.; Pople, J. A.; Head-Gordon, M. *Chem. Phys. Lett.* **1989**, *157*, 479.

(51) Boys, S. F.; Bernardi, F. *Mol. Phys.* **1970**, *19*, 553.

(52) (a) Fukui, K. *J. Phys. Chem.* **1970**, *74*, 4161. (b) Fukui, K. *Acc. Chem. Res.* **1981**, *14*, 363.

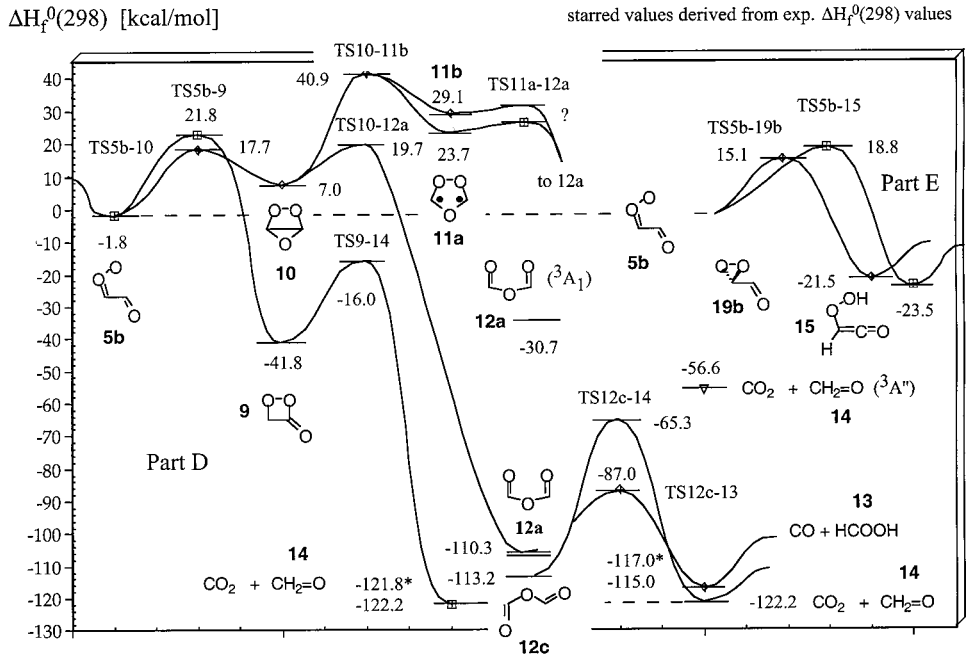

Figure 3. Energy diagram of step D of the acetylene ozonolysis (compare with Figure 1). Calculated heats of formation $\Delta H_f^0(298)$ (in kcal/mol) are given for each structure. Experimental $\Delta H_f^0(298)$ values are indicated with asterisks.

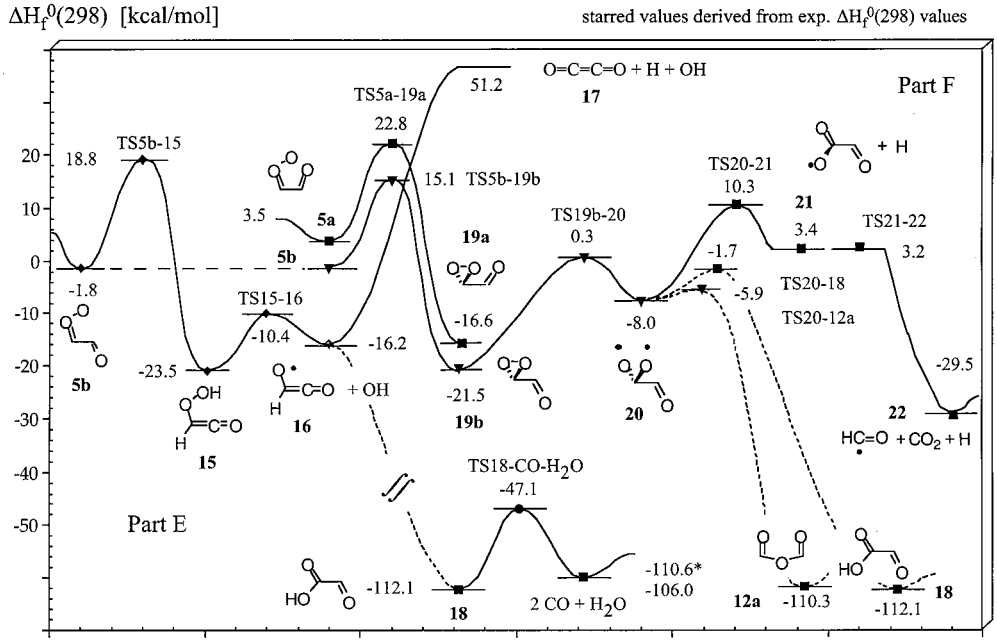

Figure 4. Energy diagram of steps E and F of the acetylene ozonolysis (compare with Figure 1). Calculated heats of formation $\Delta H_f^0(298)$ (in kcal/mol) are given for each structure. Experimental $\Delta H_f^0(298)$ values are indicated with asterisks. **TS21-22** is a TS on the PES but vanishes when ZPE correction is added.

frequencies calculated at both the CASSCF/6-31G(d,p) and the B3LYP/6-31G(d,p) levels of theory. In some cases (see text), frequency calculations were repeated with the 6-311+G(2d,2p) basis set. Frequencies were scaled by a factor of 0.8929[53] (DFT, a factor of 0.9806[54]) and used to calculate zero-point energies (ZPEs), temperature corrections, and entropies so that enthalpies at 298 K, $H(298)$, and free energies at 298 K, $G(298)$, could be determined and used to derive relative enthalpies (reaction enthalpies $\Delta_R H_f^0(298)$; activation enthalpies $\Delta H_a(298)$), which are needed for a direct comparison of quantum chemical results with measured thermochemical data. Experimental heats of formation, $\Delta H_f^0(298)$, of suitable reference molecules[55] were utilized to determine $\Delta H_f^0(298)$ values for all structures investigated, using in each case the most reliable enthalpy difference calculated. In a number of cases, suitable reference values $\Delta H_f^0(298)$ were derived from group increments[56] for comparison with the corresponding calculated data. All quantum chemical calculations were carried out using the GAMESS,[57] GAUSSIAN 94,[58] COLOGNE99,[59] and Molcas 4.1[60] program packages.

(53) Curtiss, L. A.; Raghavachari, K.; Trucks, G. W.; Pople, J. A. *J. Chem. Phys.* **1991**, *94*, 7221.

(54) Scott, A. P.; Radom, L. *J. Phys. Chem.* **1996**, *100*, 16502.

(55) (a) Cox, J. D.; Pilcher, G. *Thermochemistry of Organic and Organometallic Compounds*; Academic Press: London, 1970. (b) NIST Standard Reference Database 25, Version 2.02, National Institute of Standards and Technology, Gaithersburg. MD 20899, 1994. (c) Pedley, J. B.; Naylor, R. D.; Kirby, S. P. *Thermochemical Data of Organic Compounds*; Chapman and Hall: New York, 1986.

(56) Benson, S. W. *Thermochemical Kinetics*; John Wiley: New York, 1968.

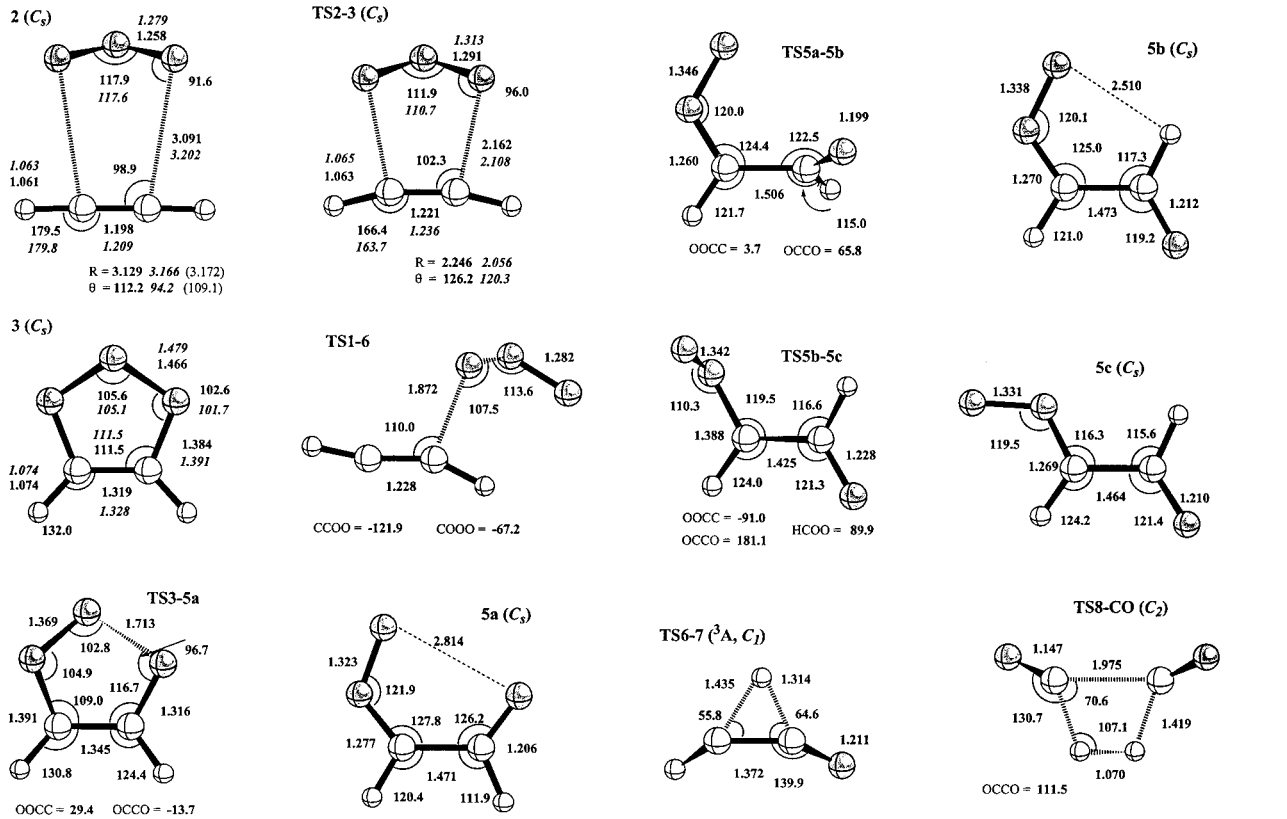

Figure 5. B3LYP/B (in bold print), CCSD(T)/B (in bold italics), and CASSCF/B geometries (in italics) of some structures encountered in steps A, B, and C of the acetylene ozonolysis. Distances in Å, angles in degrees.

4. Results and Discussions

Calculated energies, enthalpies, entropies, and dipole moments are summarized in Table 2 (for absolute energies and enthalpies, see Supporting Information). Energies and enthalpies are given relative to the corresponding values of a suitable reference structure ("ref" in Table 2) to obtain activation energies (enthalpies) and reaction energies (enthalpies). Heats of formation are calculated relative to the value of ozone + acetylene (**1**) given in line 1a (starred value) and are compared, when possible, with experimental values[55] given in the last column. On the average, calculated and experimental heats of formation differ by 2 kcal/mol (5.3% of the experimental value). This accuracy was considered to be sufficient to set up the energetics of steps A−F (Figure 1) and to represent it in Figures 2−4. Calculated geometries of molecules **1**−**22** and the corresponding TSs are shown in Figures 5−7 (Cartesian coordinates for all structures calculated are given in the Supporting Information).

In the following, we will discuss the reaction mechanism and the energetics of the ozone−acetylene reaction using preferentially calculated heats of formation to reduce, in this way, a lengthy discussion of technical aspects of the calculations (dependence of results on method and basis sets). The two basis sets used will be abbreviated as basis A (6-31G(d,p)) and basis B (6-311+G(2d,2p)). Throughout this work, geometries obtained with basis B will be discussed because they are more reliable.

(A) Formation of Trioxolene 3. The reaction between acetylene and ozone is initiated by the formation of a van der Waals complex **2**, which was verified and characterized with the help of microwave measurements and MP4 calculations.[29] B3LYP confirms the existence of a van der Waals complex, but the geometrical approach parameter *R* (distance between the center of acetylene and the midpoint between the terminal O atoms of ozone) is largely underestimated by DFT (Figure 5). A better description of the geometry of **2** is obtained at the CCSD(T)/B level of theory ($R = 3.166$ Å; experimental value, 3.172 Å;[29] Figure 5), which is also reflected in the calculated C,O distances (3.202 vs 3.209 Å,[29] Figure 5). It is well-known that standard DFT functionals fail to correctly describe van der Waals complexes[61,62] and loose TSs[63] in the way that they exaggerate the stability of the TS and predict false van der Waals complexes too close to the TS.[64] This is also found in the present case; therefore, only the CCSD(T)/B results will be discussed in the following. After BSSE corrections, van der Waals complex **2** is 1.1 kcal/mol more stable than the separated molecules (Table 2), which is reasonable in view of the fact

(57) Schmidt, M. W.; Baldrige, K. K.; Boatz, J. A.; Jensen, J. H.; Koseki, S.; Gordon, M. S.; Nguyen, K. A.; Windus, T. L.; Elbert, S. T. *QCPE Bull.* **1990**, *10*, 52.

(58) Frisch, M. J.; Trucks, G. W.; Schlegel, H. B.; Scuseria, G. E.; Robb, M. A.; Cheeseman, J. R.; Zakrzewski, V. G.; Montgomery, J. A., Jr.; Stratmann, R. E.; Burant, J. C.; Dapprich, S.; Millam, J. M.; Daniels, A. D.; Kudin, K. N.; Strain, M. C.; Farkas, O.; Tomasi, J.; Barone, V.; Cossi M.; Cammi, R.; Mennucci, B.; Pomelli, C.; Adamo, C.; Clifford, S.; Ochterski, J.; Petersson, G. A.; Ayala, P. Y.; Cui, Q.; Morokuma, K.; Malick, D. K.; Rabuck, A. D.; Raghavachari, K.; Foresman, J. B.; Cioslowski, J.; Ortiz, J. V.; Stefanov, B. B.; Liu, G.; Liashenko, A.; Piskorz, P.; Komaromi, I.; Gomperts, R.; Martin, R. L.; Fox, D. J.; Keith, T.; Al-Laham, M. A.; Peng, C. Y.; Nanayakkara, A.; Gonzalez, C.; Challacombe, M.; Gill, P. M. W.; Johnson, B.; Chen, W.; Wong, M. W.; Andres, J. L.; Gonzalez C.; Head-Gordon, M.; Replogle, E. S.; Pople, J. A. *Gaussian 98*, Revision A.5; Gaussian, Inc.: Pittsburgh, PA, 1998.

(59) Kraka, E.; Gräfenstein, J.; Gauss, J.; Reichel, F.; Olsson, L.; Konkoli, Z.; He, Z.; Cremer, D. COLOGNE 99, Göteborg University, Göteborg, 1999.

(60) Anderson, K.; Fülscher, M. P.; Lindh, R.; Malmqvist, P. A.; Olsen, J.; Roos, B. O.; Sadlej, A. J.; Widmark, P. O. MOLCAS Version 4, University of Lund and IBM, Lund, Sweden 1991.

(61) Kristyan, S.; Pulay, P. *Chem. Phys. Lett.* **1994**, *229*, 175.

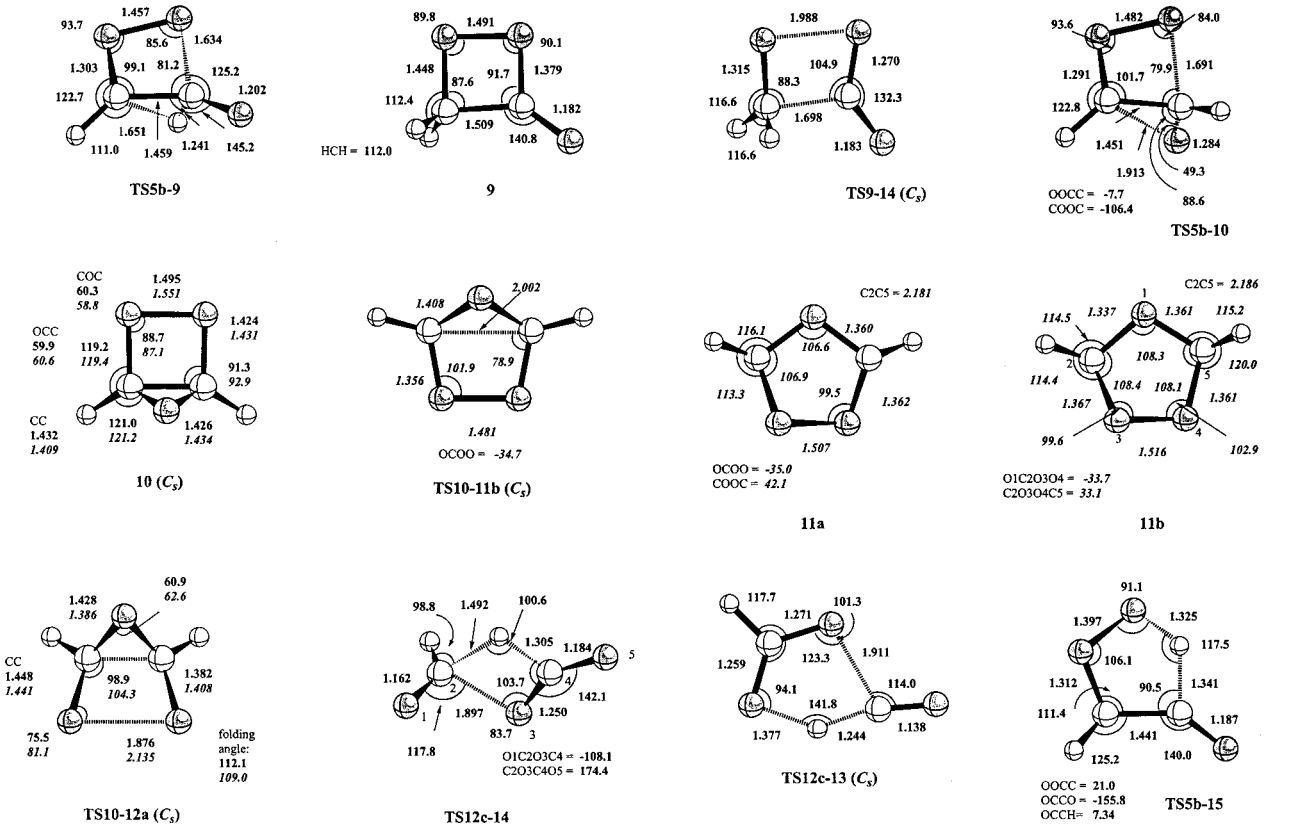

Figure 6. B3LYP/B (in bold print) and CASSCF/B geometries (in italics) of some structures encountered in step D of the acetylene ozonolysis. Distances in Å, angles in degrees.

that the complex could be observed by microwave spectroscopy.[29]

In analogy to the $[4\pi + 2\pi]$ cycloaddition reaction between ozone and ethene, the formation of 1,2,3-trioxolene (**3**) should occur in a concerted step, in line with the Woodward−Hoffmann rules.[65] An alternative two-step mechanism via an open-shell singlet biradical **4** was suggested by DeMore,[3] who argued that the *A* factor obtained for the ozone−acetylene reaction in rate constant measurements can be explained only by considering **4** as an intermediate. An intensive search for both **4a** and **4b** (see Figure 1) at the CASSCF and UDFT levels of theory carried out in this work provided no clue for a local minimum on the PES occupied by **4**. On the other hand, **TS2-3** of the formation of **3** is typical of a concerted reaction step. The approach parameter *R* decreased to 2.06 Å, equivalent to CO distances of 2.11 Å (see Figure 5). The CC and OO bonds are slightly lengthened, but the overall features of the van der Waals complex **2** are largely retained in **TS2-3**.

According to CCSD(T)/B calculations, the activation enthalpy is 9.6 kcal/mol (measured with respect to the van der Waals minimum), which compares well with $\Delta H_a(298) = 10.2 \pm 0.4$ kcal/mol (Arrhenius energy $E_a = 10.8 \pm 0.4$ kcal/mol), as measured by DeMore.[3] Hence, $\Delta H_a(298)$ of the $[4\pi + 2\pi]$ cycloaddition reaction between ozone and acetylene is about twice as large as the activation enthalpy of the ozone−ethene cycloaddition reaction (4.7 kcal/mol[3]). The increase in the barrier is a direct result of the greater strength of the triple bond and the lower availability of the π electrons of the CC bond in acetylene. According to the frontier orbital theory of Fukui,[66] the barrier is influenced by orbital interactions between the HOMO and the LUMO of the reactants, which decrease with a lowering of the HOMO of the unsaturated hydrocarbon. For ethene, the measured first ionization potential (IP) is 10.5 eV, while the corresponding IP value for acetylene is 11.4 eV.[67] Hence, calculated and measured activation enthalpy are in line with FMO theory.

Additionally, the calculated entropy *S* of **TS2-3** (70.7 eu, Table 2) is in line with the prediction made by DeMore (69 eu).[3] It reveals that the large *A* factor of $10^{9.5}$ is a direct consequence of the existence of a van der Waals complex. The activation entropy ΔS_a is reduced from $(70.7 - 104.6) = -33.9$ eu to $(70.7 - 86.5) = -10.2$ eu, and a large *A* factor is obtained. This point was overlooked by DeMore,[3−5] and, accordingly, there is no need to invoke an intermediate biradical such as **4**.

The reaction enthalpy $\Delta_R H(298)$ of the formation of **3** is −57.8 kcal/mol (relative to **2**, Table 2), which means that **3** is formed with an excess energy of 67 kcal/mol and should represent in the gas phase a vibrationally excited (*hot*) molecule. If **3** could be cooled in solution phase by energy dissipation, then it would exist in an envelope form (folding angle 151°; see Figure 5). The planar form, which corresponds to the TS of ring inversion, is less stable by just 0.4 kcal/mol. Molecule **3** is characterized by an antiaromatic 8π system; therefore, **3** should be significantly destabilized. Utilizing reaction 1, which should

(62) (a) Hobza, P.; Sponer, J.; Reschel, T. *J. Comput. Chem.* **1995**, *16*, 1315. (b) Ruiz, E.; Salahub, D. R.; Vela, A. *J. Am. Chem. Soc.* **1995**, *117*, 1141.

(63) (a) Johnson, B. G.; Gonzales, C. A.; Gill, P. M. W.; Pople, J. A. *Chem. Phys. Lett.* **1994**, *221*, 100. (b) Baker, J.; Muir, M.; Andzelm, J. *J. Chem. Phys* **1994**, 102, 2063. (c) Baker, J.; Andzelm, J.; Muir, M.; Taylor, P. R. *Chem. Phys. Lett.* **1995**, *237*, 53.

(64) Wrobel, R.; Sander, W.; Kraka, E.; Cremer, D. *J. Phys. Chem. A* **1999**, *103*, 3693.

(65) See, e.g.: Woodward, R. B.; Hoffmann, R. *Angew. Chem., Int. Ed. Engl.* **1969**, *8*, 781.

(66) Fukui, K. *Angew. Chem., Int. Ed. Engl.* **1982**, *21*, 801.

(67) *CRC Handbook of Chemistry and Physics on CD-ROM*, 2000 Version; Lide, D. R.,Ed.; CRC Press LLC: Boca Raton, FL, 2000.

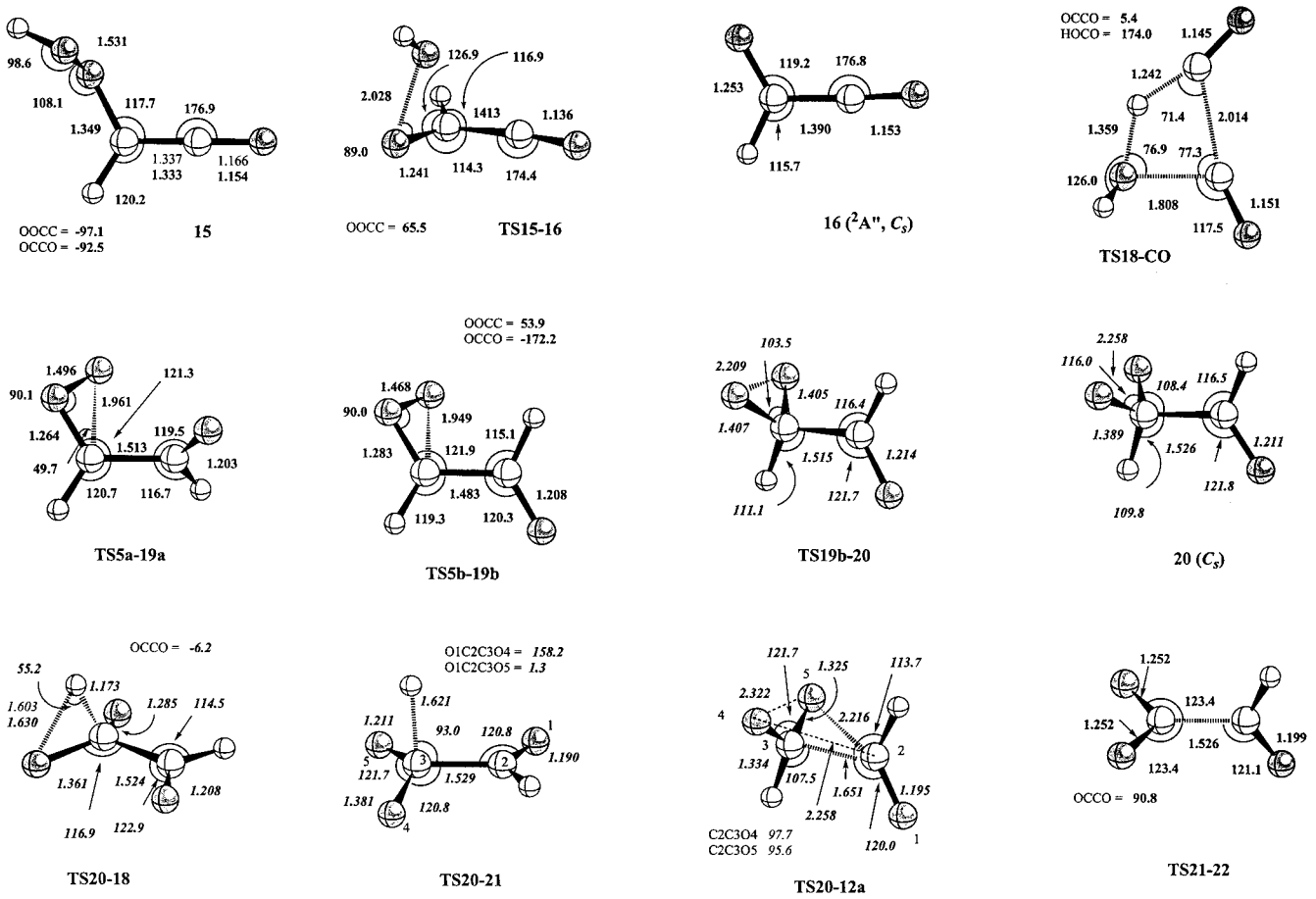

Figure 7. B3LYP/B (in bold print) and CASSCF/B geometries (in italics) of some structures encountered in steps E and F of the acetylene ozonolysis. Distances in Å, angles in degrees.

be balanced with respect to the ring strain energies of the molecules involved,[68] the destabilization of **3** is calculated to be 8.9 kcal/mol.

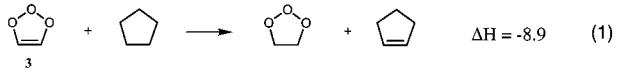

(B) α-Keto Carbonyl Oxide 5. A concerted cycloreversion of primary ozonide **3** involves the cleavage of the OO and the CC π bonds, where the latter can be considered as a consequence of the OO cleavage because it corresponds actually to a reorganization of the π electrons (reaction 2).

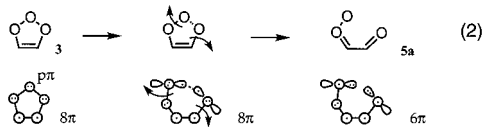

In contrast to the cycloreversion of an alkene primary ozonide, the resulting carbonyl oxide and aldehyde are connected by a CC single bond. Hence, concerted and nonconcerted primary ozonide decompositions collapse in the case of the acetylene ozonolysis to one possible reaction path, namely the formation of **5**. The activation enthalpy $\Delta H_a(298)$ for reaction 2 is 4.3 kcal/mol, while the calculated reaction enthalpy $\Delta_R H(298)$ is −27.0 kcal/mol (Table 1); i.e., carbonyl oxide **5** is significantly more stable than trioxolene **3**. As shown in Scheme 2, there are four possible forms of **5**, which all occupy local minima on the PES. The cis,syn form **5a**, which is formed in the ring-opening reaction 2, is 5.3 kcal/mol less stable than the cis,anti form **5b**. It is noteworthy that the activation enthalpy for rotation at the CC bond is just 2.7 kcal/mol, where in **TS5a-5b** the aldehyde group is rotated by just 65.8° (Figure 5), rather than 90° as one might expect. **5b** benefits from more favorable dipole−dipole interactions between aldehyde and carbonyl oxide groups. However, optimal dipole−dipole interactions are accomplished in the trans,anti form **5c**, which is 2.5 and 7.8 kcal/mol more stable than forms **5b** and **5a**, respectively (Scheme 2, Table 1). The activation enthalpy for cis−trans isomerization (**TS5b-5c**) is 17.5 kcal/mol, which is considerably smaller than the activation enthalpy for the parent carbonyl oxide (26 kcal/mol)[32] and again a consequence of π-conjugation in **5**. Rotation at the CC bond leads to the trans,syn form **5d**, which is 3.8 kcal/mol less stable than **5c**.

The rotational barrier given by the energy of **TS5c-5d** (11.4 kcal/mol; $\Delta H_a(298) = 10.4$ kcal/mol, Table 2, Scheme 2, Figure 5) provides a measure for the degree of π-delocalization in **5c**, which is larger than that in 1.3-butadiene (7.3 kcal/mol)[69] due to the extension from 4π to 6π electrons. In Scheme 2 (reactions 3−10), **5c** is related to *trans*-acrolein and *trans*-glyoxal, which in turn are related to *trans*-1,3-butadiene by formal reactions 7−10. The bond separation energy of the latter molecule is 14.6 kcal/mol, half of which is due to π-delocalization, while the other half results from changes in bond lengths if standard single and double bonds are incorporated into a conjugated system.[69a]

(68) Cremer, D. *Isr. J. Chem.* **1983** *23*, 72.

(69) (a) Kraka, E.; Cremer, D. *J. Mol. Struct. (THEOCHEM)* **2000**, *506*, 191. (b) Roth, W. R.; Adamczak, O.; Breuckmann, R.; Lennartz, H. W.; Boese, R. *Chem. Ber.* **1991**, *124*, 2499.

Scheme 2

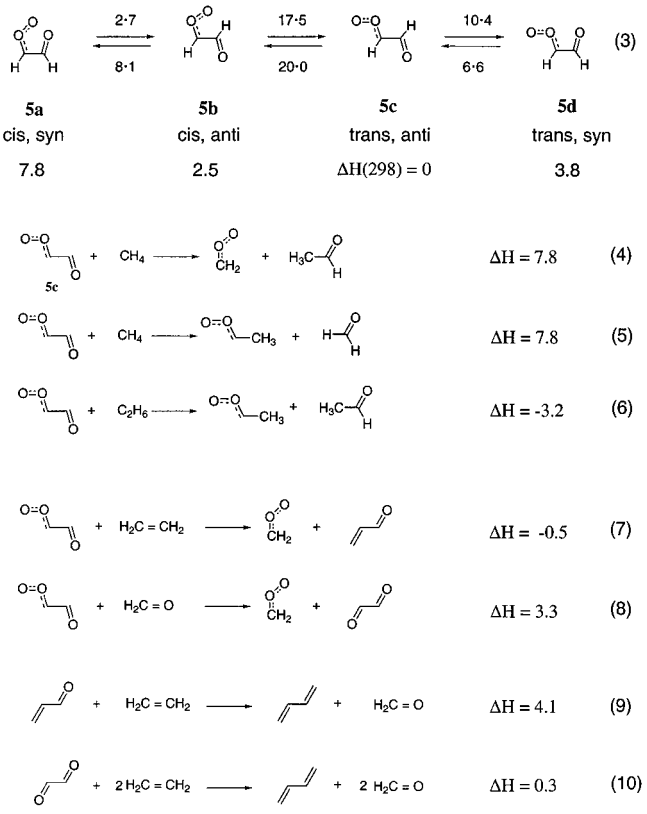

Hence, the bond separation enthalpies of *trans*-acrolein, *trans*-glyoxal, and **5c** are 18.7 (14.6 + 4.1; reaction 9), 14.9 (14.6 + 0.3; reaction 10), and 18.2 kcal/mol (reactions 7 and 9, 18.7−0.5; reactions 8 and 10, 14.9 + 3.3), respectively. The stabilization of carbonyl oxide by an aldehyde group (18.2 kcal/mol) is considerably larger than that caused by a methyl group (7.8 − 18.2 = −10.4 kcal/mol, reaction 5 in Scheme 2; compare also with reactions 4 and 6) Clearly, the higher stability of α-keto carbonyl oxide **5** will lead to a longer lifetime and, under certain conditions, to a larger selectivity in its reactions.

(C) Decomposition of α-Keto Carbonyl Oxide 5 by Oxygen Loss. In view of the large excess energy of 100 kcal/mol (difference between the energies of **TS2-3** and **5b**), generated in the gas-phase formation of **5**, its lifetime will be rather short in the gas phase, where the chance of energy dissipation by collisions is small. Even high-energy processes such as loss of $O_2(^1\Delta_g)$ (according to spin conservation rules) leading to carbene **6** ($\Delta_R H(298)$ = 88.8 kcal/mol, Table 2, Figure 2) cannot be excluded.

As an alternative route for the formation of carbene **6**, we found that an O-transfer via **TS1-6** can take place (activation enthalpy, 15.6 kcal/mol, Table 2, Figure 2) according to reaction 11. IRC calculations reveal that carbene **6** and O_2 are formed

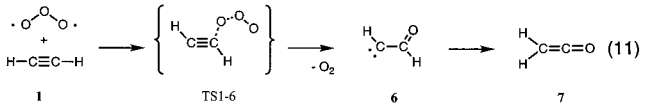

in their triplet states ($\Delta_R H_f^0(298)$ = −37.4 kcal/mol, Table 2) rather than the corresponding combination of singlet states, which is 35.9 kcal/mol higher in energy (Figure 2). Rearrangement of **6** to oxirene is a low-energy process and has been discussed in detail in the literature.[70−72] However, oxirene will easily revert to **6**; therefore, the oxirene route was not further investigated in this work. H migration and rearrangement of **6** to ketene **7** in its triplet state requires 39.2 kcal/mol but should be possible in the gas phase in view of an excess energy of more than 50 kcal/mol. However, the same reaction would not be possible on the singlet PES (leading to the ground state of **7**) because the corresponding TS ($\Delta H_f^0(298)$ = 107.2 kcal/mol, Figure 2) would be above **TS1-6**.[73]

Cleavage of the OO bond in **5b** (**5c**), thus leading to either to $O(^1D)$ and glyoxal (**8**) in its ^1A_g ground state or $O(^3P)$ and the excited ^3A_u state of **8** according to spin conservation rules, requires just 53.0 (55.5) and 52.0 (54.5) kcal/mol, respectively, and, therefore, is equally likely as cleavage of the CO bond and loss of O_2. Subsequent decomposition of **8** on the singlet PES via **TS8-CO** ($\Delta H_a(298)$ = 57.2 kcal/mol) is too high in energy to take place within the acetylene ozonolysis. Hence, a loss of atomic or molecular oxygen in **5** will preferentially lead to **8** and, to a minor extent, **7**.

(D) Cyclization of α-Keto Carbonyl Oxide 5. H transfer in form **5b** leads to ring closure and the formation of a planar 3-keto-1,2-dioxetane (dioxetanone **9**, see Figure 1) in a concerted process involving a nucleophilic attack of the terminal O atom of the carbonyl oxide group at the aldehyde carbon (see **TS5b-9** in Figure 6). The activation enthalpy for this process is just 23.6 kcal/mol, and the reaction enthalpy (relative to **5b**) is −40 kcal/mol (Table 2, Figure 3), where the exothermicity is a result of the formation of a new CO bond. Nevertheless, **9** is heavily strained, which is reflected by an unusually long OO bond (1.491 Å, Figure 6) compared to a typical peroxide bond length of 1.45 Å.[74] Dioxetanone **9** can decompose to formaldehyde and CO_2 with a calculated activation enthalpy of 25.8 kcal/mol, which is typical of the thermolysis of dioxetanes and dioxetanones (25 ± 5 kcal/mol).[75] Actually, the process leading to the $^1A_1$ ground state of CH_2═O ($\Delta_R H(298)$ = −80.4 kcal/mol, Table 2, Figure 3) is symmetry forbidden, and by spin inversion the $^3A''$ state of CH_2═O is formed (excitation energy, 72 kcal/mol;[76] calculated, 66 kcal/mol; $\Delta_R H(298)$ = −14.8 kcal/mol; corrected considering the error in the calculated excitation energy, − 9 kcal/mol). The nature of this process is reflected by the calculated geometry of **TS9-14** (Figure 6) obtained at the UB3LYP level of theory since the corresponding RB3LYP solution is unstable by 1.2 kcal/mol. Decomposition of the dioxetanone ring is initiated by OO bond lengthening and the generation of a biradical with considerable spin−orbit coupling that makes possible a spin flip and change to the triplet PES.[77] The subsequent breakage of the CC bond starts at the TS, which is nicely reflected by the calculated OO (1.988 Å, bond already broken) and CC distances (1.698 Å, bond starting to break, UB3LYP/B results, Figure 6). Delocalization of the single electrons at the O atoms into the π and π^* orbitals of the C═O fragments being formed reduces spin−orbit coupling and, by

(70) Scott, A. P.; Nobes, R. H.; Schaefer, H. F., III; Radom, L. *J. Am. Chem. Soc.* **1994**, *116*, 10159.
(71) Parker, J. K.; Davies, S. R. *J. Phys. Chem. A* **1999**, *103*, 7280.
(72) Bachmann, C.; McGuessan, T. Y.; Debu, F.; Monnier, M.; Pourcin, J.; Aycard, J.-P.; Bodot, H. *J. Am. Chem. Soc.* **1990**, *112*, 7488.
(73) We note that the activation enthalpy for the rearrangement **6** → **7** on the singlet PES is in line with the value given in ref 70, while in ref 71 a value of just 1.9 kcal/mol is given.
(74) Cremer, D. In *The Chemistry of Functional Groups, Peroxides*; Patai, S., Ed.; Wiley: New York, 1983; p 1.
(75) (a) Adam, A. *Adv. Heterocycl. Chem.* **1988**, *21*, 437. (b) Wilson, T. *International Review of Science, Physical Chemistry*; London, Butterworth: 1976; Series Two, Vol. 9, p 265.
(76) Herzberg, G. *Molecular Spectra and Molecular Structure, III. Electronic Spectra and Electronic Structure of Polyatomic Molecules*; van Nostrand Reinhold Co.: New York, 1966.
(77) Turro, N. J. *Modern Molecular Photochemistry*; University Science Books, Sausalito, CA, 1991.

this, the possibility of returning to the singlet PES. Hence, the decomposition of **9** should be a typical chemiexitation process accompanied by chemiluminescence.[77]

The second possible cyclization process of **5b** leads to 2,3,5-trioxabicyclo[2.1.0]pentane (**10**), which can be considered as the final ozonide (1,2,4-trioxolane found in the ozonolysis of alkene) of the ozonolysis of acetylene. However, in contrast to the normal formation of final ozonides, **10** is formed by intramolecular substitution (nucleophilic attack of the terminal O atom at the carbonyl C and cleavage of the C═O π-bond, **TS5b-10**, see Figure 6), similar to the case of **9**, rather than by $[4\pi + 2\pi]$ cycloaddition. The formation of ozonide **10** is a concerted but rather asynchronous process, which is reflected by the difference in the C,O distances of **TS5b-10** (1.691 and 1.913 Å, Figure 6). Hence, the driving force for the ozonide formation is the nucleophilic attack of the terminal O atom of the carbonyl oxide moiety at the aldehyde C, which is followed by the breaking of the C═O double bond, pyramidalization of the aldehyde group, and the epoxide formation. The activation enthalpy and reaction enthalpy of the formation of **10** are calculated to be 19.5 and 8.8 kcal/mol, respectively (Table 2, Figure 3). The existence of **10** was verified by Ando et al.;[10] however, its properties are not known. Molecule **10** possesses an envelope form, and its OO bond is lengthened in a way similar to that in **9**. The CC bond (1.432 Å, Figure 6) is almost 0.1 Å longer than that in its homologue dioxetene (1.338 Å, HF/6-31G(d,p))[78] but 0.1 Å shorter than that in **9**. Ozonide **10** is 48.8 kcal/mol less stable than dioxetanone **9**, which is due to the loss of the C═O aldehyde bond and the extra strain introduced by the epoxide ring and the bicyclic structure.

As a dioxetane, **10** should decompose in a way similar to the decomposition of **9**, which is confirmed by the geometry of **TS10-12a**. The OO bond is elongated to 1.88 Å (B3LYP/B), while the CC bond hardly changes (1.448 compared to 1.432 Å, Figure 6). At the CASSCF(8,8)/B level of theory, the difference between CC and OO distances (1.441 vs 2.135 Å) is even stronger, suggesting that at the TS essentially a dialkoxy biradical (DAB) exists.

Following the IRC of the reaction path from **TS10-12a** into both the entrance and the exit channels, it was possible to clarify that the TS calculated directly connects ozonide **10** and formanhydride **12a** without any intermediate related to biradical DAB and a second TS, in which the CC bond is broken. Hence, a stepwise decomposition process to avoid the symmetry-forbidden thermolysis of the dioxetane ring of **10** can be ruled out. Therefore, it is likely that the mechanism discussed for the decomposition of **9** also applies to **10** and that anhydride **12a** is formed with an activation enthalpy $\Delta H_a(298) = 12.7$ kcal/mol (Table 2, Figure 3) in a triplet state ($\Delta_R H(298) = -37.7$ kcal/mol; T-excitation enthalpy of **12a**, 79.6 kcal/mol, Table 2) rather than its singlet ground state ($\Delta_R H(298) = -117.3$ kcal/mol).

An isomer of ozonide **10** is the biradical **11**, which can be formed by either a conrotatory or (inward-directed) disrotatory ring-opening process, although the former process should be slightly preferred because the oxirane ring opening is symmetry-allowed in the conrotatory mode (see Scheme 3). The latter process leads to the C_2-symmetrical biradical **11a** (C···C = 2.181 Å, Figure 6), while the disrotatory process (**TS10-11b** C···C, 2.002 Å, Figure 6) generates the C_s-symmetrical biradical **11b** (C···C = 2.186 Å, Figure 6). The value of $\Delta H_a(298)$ for the formation of **11b** is 33.9 kcal/mol (Figure 3), which is considerably larger than the corresponding value for the rearrangement to **12a**. In analogy to ethene final ozonide,[68,79] which prefers C_2 symmetry because of the gauche preference of peroxide molecules,[74,80] form **11a** is 5.4 kcal/mol more stable than **11b**. Biradical **11b** is 22.1 kcal/mol higher in enthalpy than isomer **10**. It can decompose either by OO bond cleavage to anhydride **12a** or via CO bond cleavage to the peroxycarbene (POC) of Scheme 3. An intensive search for the TS of the first reaction at CASSCF and UB3LYP was unsuccessful but revealed that the barrier to OO bond cleavage must be lower than 2 kcal/mol. The second path was not investigated because the formation of anhydride **12a** should preferentially proceed via **TS10-12a**.

Scheme 3

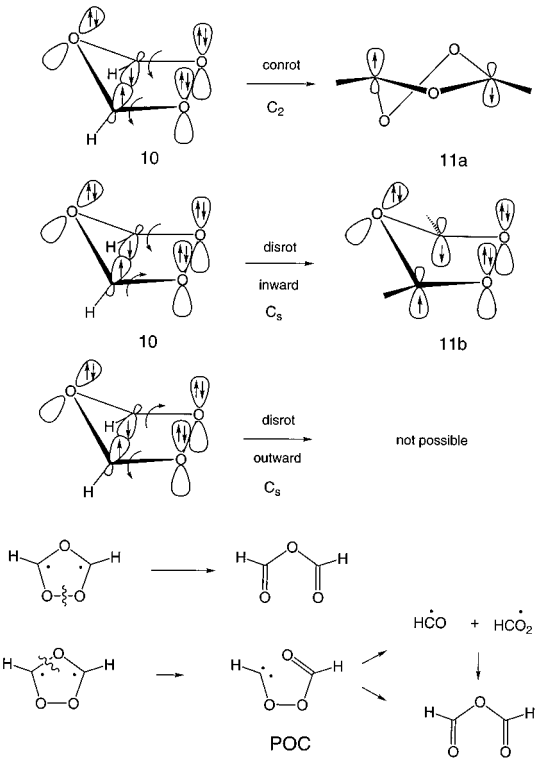

There exist three conformations of **12**, of which **12c** provides the arrangement of C═O bond dipoles with the least destabilizing interaction and, therefore, is 2.7 and 2.9 kcal/mol more stable than **12b** and **12a**, respectively. This is of little relevance, considering that **12** is formed with an excess enthalpy of at least 130 kcal/mol (relative to **10**). This enthalpy is sufficient for a rapid decomposition into either CO + HCOOH (**13**) or CO_2 + H_2CO (**14**), where both processes start from conformation **12c**. The former process requires a H transfer from C to a keto O atom and cleavage of an ether linkage (see **TS12c-13** in Figure 6). The values of $\Delta H_a(298)$ and $\Delta_R H_f^0(298)$ are 26.2 and −2.0 kcal/mol, which makes this process more likely than the second decomposition path. The latter implies H transfer to a carbonyl C and breakage of the adjoint ether linkage (see **TS12c-14**, Figure 6). The corresponding $\Delta_R H(298)$ and $\Delta H_a(298)$ values are 47.9 and −9.0 kcal/mol. Formic acid can further decompose to H_2O, CO, H_2, or CO_2.[31]

(78) Budzelaar, P. H. M.; Kraka, E.; Cremer, D.; Schleyer, P. v. R. *J. Am. Chem. Soc.* **1986**, *108*, 561.

(79) (a) Cremer, D. *J. Chem. Phys.* **1978**, *70*, 1898. (b) Cremer, D. *J. Chem. Phys.* **1979**, *70*, 1928.

(80) Cremer, D. *J. Chem. Phys.* **1978**, *69*, 4440.

(E) Possibility of OH Production. For the gas-phase ozonolysis of alkenes, the formation of OH radicals was verified by a combination of kinetic measurements, ab initio calculations, and RRKM investigations.[21,22] Recently, OH generation from carbonyl oxides via H migration, hydroperoxide formation, and OO bond rupture was also confirmed for the solution phase.[81,82] Accordingly, it was checked whether OH production is also possible in the acetylene ozonolysis.

In α-keto carbonyl oxide **5b**, an H atom is located in such a position that it can be transferred via a 1,4-shift to the terminal O atom of the carbonyl oxide group, thus leading to the hydroperoxyl ketene **15**. The **TS5b-15** possesses geometrical features (see Figure 6) similar to those found for the H shift of methyl−carbonyl oxide,[21] while the calculated $\Delta H_a(298)$ value of 20.6 kcal/mol (Table 2, Figure 4) is slightly higher, but competes well with the formation of ozonide **10** (19.5 kcal/mol) or dioxetanone **9** (23.6 kcal/mol, see Table 2). The ketene **15** is 21.7 kcal/mol more stable than the carbonyl oxide **5b**.

The excess enthalpy of **15** in the gas phase is at least 42 kcal/mol (relative to the energy of **TS5b-15**), which is sufficient to break the OO bond. Normally such a dissociation process occurs without a barrier; however, in the case of a larger reorganization of the electronic structure an energy barrier may develop.[82] In the case of **TS15-16** (see Figure 7), the single electron is generated in a π-orbital which is part of an oxallyl unit; therefore, it can delocalize, thus leading to spin density at the C atom (see structure **16b**). The calculated $\Delta H_a(298)$ value for OO cleavage is 13.1 kcal/mol, and the reaction enthalpy 7.3 kcal/mol.

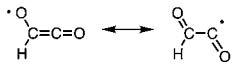

16a 16b

The calculated geometry of **16** (CC bond, 1.390; OC(H) bond, 1.253 Å, Figure 7) confirms that both resonance structures contribute to its wave function. Recombination with an OH radical (e.g., if the latter is formed in a solvent cage) to yield **15** requires a destruction of the partial double bond character of the OC(H) bond and implies, therefore, a reaction barrier of 5.8 kcal/mol, while attack of the OH group at the C atom leads to a strongly exothermic reaction ($\Delta_R H(298) = -95.9$ kcal/mol, Table 2) without any barrier, yielding glyoxylic acid (**18**, Figure 4). −CH bond cleavage in **16**, leading to **17**, requires spin inversion and a large enthalpy of 67.8 kcal/mol, which makes this process unlikely. Product **17** has a triplet ground state (in analogy to O_2), while the first excited singlet state dissociates to two CO molecules.

(F) Dioxirane Formation. Carbonyl oxides are known to isomerize to dioxiranes,[83,84] which are normally much more stable than their acyclic counterparts.[31] Ring opening of a dioxirane leads to a bisoxy biradical and different rearrangement and decomposition products derived from the biradical (refs 31, 32, and references therein). Compared to the parent carbonyl oxide, the activation enthalpy for cyclization (16.9 kcal/mol, **TS5b-19**, Figures 4 and 7) is 2 kcal/mol smaller. Cyclization of **5a**, however, requires 19.3 kcal/mol due to the steric interactions between aldehyde group and the ring in the TS (see **TS5a-19a**, Figure 7) when forming the gauche conformation of dioxirane **19**.

Ring opening of **19** requires an activation enthalpy of 21.8 kcal/mol and leads to the bisoxy biradical **20** in an endothermic reaction ($\Delta_R H_f^0(298) = 13.5$ kcal/mol, Table 2, Figure 4). These values are in line with the values found for methyl- and dimethyl-substituted methylenebis(oxy) biradicals ($\Delta H_a(298) =$ 22.2 and 23.1 kcal/mol; $\Delta_R H_f^0(298) = 7.0$ and 11.1 kcal/mol).[31] Steric repulsion between the substituents at C leads to a reduction of the OCO angle (**20**, Figure 7, 116.0°; dimethyl derivative, 117.8°; parent molecule, 125.0°)[31] and an increase of lone pair−lone pair repulsion, thus raising the energy of the TS and the biradical (parent molecule, $\Delta H_a(298) = 18.0$; $\Delta_R H_f^0(298) = 1.2$ kcal/mol).[31]

Biradical **20** is a minimum at the CASSCF level (Table 2), but single-point CASPT2//CASSCF calculations for **TS20-12a** and **TS20-18** suggest that **20** does not exist. Since such discrepancies are often encountered when CASPT2 energies are determined for CASSCF geometries because of the inaccuracy of the latter, in particular for loose TSs, and since CASPT2 geometry optimizations are not feasible, we conclude that the rearrangements of biradical **20** are better described at the CASSCF level.

Three-electron interactions between the σ(CC) electron pair and the single electrons of methylenebis(oxy) biradical **20** (partial occupation of the σ^*(CC) orbital) enhanced by the inductive effects of the O atoms lead to a significant lengthening of the CC bond (1.526 Å, Figure 7), which was also found for other methylenebis(oxy) biradicals.[31] The weakening of the CC bond is the reason for the facile migration ($\Delta H_a(298) = 2.1$ kcal/mol, **TS20-12a**, Table 2, Figure 7) of the aldehyde group to one of the O atoms, thus yielding anhydride **12a**.

H rather than CH═O migration ($\Delta H_a(298) = 6.3$ kcal/mol, Table 2, Figure 4; **TS20-18**, Figure 7) leads to glyoxylic acid **18**. H abstraction from **20** (**TS20-21**, Figure 7) requires an activation enthalpy $\Delta H_a(298) = 18.3$ kcal/mol (parent molecule, 18.4 kcal/mol)[24] and yields the acyl radical **21** in an endothermic process (Table 2). Radical **21** is not stable and decomposes without an activation enthalpy ($\Delta E = 1.1$; $\Delta H_a(298) = -0.2$ kcal/mol, Table 2; **TS21-22**, Figure 7) to CO_2, a H atom, and the formyl radical **22** in an exothermic reaction ($\Delta_R H(298) =$ −32.9 kcal/moll). We did not find a TS for the decomposition of biradical **20** into CO_2 and H_2C═O, which should require a large activation enthalpy, such as that found for methyl-substituted biradicals.[31]

In view of the relatively small barrier to CH═O migration, the lifetime of biradical **20** should be very small. Nevertheless, the biradical plays an important role in part F of the reaction mechanism because its decomposition barriers determine that anhydride **12**, along with some acid **18**, is the major product once dioxirane is formed in the acetylene ozonolysis (Figure 1).

5. Chemical Relevance of Results

This work leads to a number of chemically interesting insights into the reaction mechanism of the ozonolysis of acetylene in particular and alkynes in general:

(1) The formation of trioxolene **3** takes place as a concerted symmetry-allowed [$4\pi + 2\pi$] cycloaddition reaction, which starts at van der Waals complex **2**. The calculated geometry for **2** agrees well with the corresponding microwave structure of Gillies and co-workers.[29] Theory predicts that a two-step

(81) (a) Kirschfeld, A.; Muthusamy, S.; Sander, W. *Angew. Chem.* **1994**, *106*, 2261; *Angew. Chem., Int. Ed. Engl.* **1994**, *33*, 2212. (b) Sander, W.; Kirschfeld, A.; Kappert, W.; Muthusamy, S.; Kiselewsky, M. *J. Am. Chem. Soc.* **1996**, *118*, 6508.

(82) (a) Kraka, E.; Sosa, C. P.; Cremer, D. *Chem. Phys. Lett.* **1996**, *260*, 43. (b) Sander, W.; Block, K.; Kappert, W.; Kirschfeld, A.; Muthusamy, S.; Schroeder, K.; Sosa, C. P.; Kraka, E.; Cremer, D. *J. Am. Chem. Soc.* **2001**, *123*, 2618.

(83) Bunnelle, W. H. *Chem. Rev.* **1991**, *91*, 335.

(84) Sander, W. *Angew. Chem., Int. Ed. Engl.* **1989**, *29*, 344.

Scheme 4

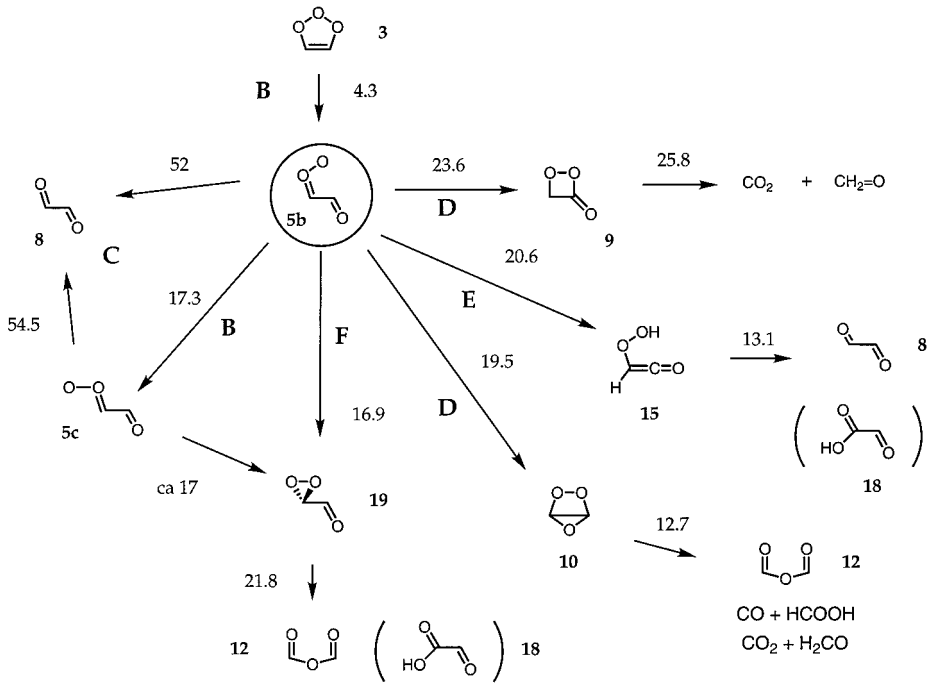

mechanism with a biradical intermediate **4** (Figure 1) is unlikely and that the experimental evidence in favor of a two-step mechanism actually confirms the existence of complex **2** rather than that of an intermediate biradical **4**. The large *A* factor of $10^{9.5}$ measured by DeMore[3] shows that the activation entropy ΔS_a is relatively small, which is a necessary consequence of the fact that ΔS_a has to be determined as $S(\mathbf{TS2\text{-}3}) - S(\mathbf{2}) = -15.8$ eu (Table 1) rather than $S(\mathbf{TS2\text{-}3}) - S(\mathbf{1}) = -33.9$ eu. At CCSD(T)/B, the calculated activation enthalpy of 9.6 kcal/mol is in good agreement with the corresponding experimental value of 10.2 kcal/mol (Arrhenius activation energy, 10.8 kcal/mol).[3]

(2) The activation enthalpy for the formation of **3** is considerably higher than that for the formation of ethene primary ozonide (4.7 kcal/mol[3]). This can be explained with the help of FMO theory: the energy of the HOMO of acetylene is considerably lower than that of the HOMO of ethene, which is reflected by the ionization potentials of acetylene and ethene (11.4 vs 10.5 eV).[67] In this way, stabilizing two-electron HOMO−LUMO interactions between the reactants are smaller in the case of acetylene. In alkyl-substituted acetylenes, the IP decreases below that of ethene (e.g., 1-octyne, 9.95; 2-octyne, 9.31; 3-octyne, 9.22; 4-octyne, 9.20 eV);[67] therefore, one can predict that activation enthalpies are much lower in these cases than in the case of acetylene.

(3) Besides the $[4\pi + 2\pi]$-cycloaddition reaction, ozone can also act as an O-transfer agent, yielding ketene via the intermediate carbene **6**. The corresponding activation enthalpy (15.6 kcal/mol, Table 1, Figure 2) is just 5 kcal/mol larger than that for the cycloaddition reaction. We note that recently Parker and Davies[71] found ketene in low-temperature studies of the ozonolysis of dimethylacetylene. The authors explained the formation of ketene as a consequence of the reaction of atomic oxygen (generated by the decomposition of ozone) and acetylene. In view of the results obtained in this work, ketene can also (or preferentially) be formed by a direct reaction of ozone with an alkyne.

(4) There is no calculational support for previous arguments by Keay and Hamilton[6,7] that **3** is more stable than carbonyl oxide **5** and that because of this **3** must be one of the epoxidation agents generated in the acetylene ozonolysis. On the contrary, **3** is destabilized by about 9 kcal/mol due to an antiaromatic 8π electron ensemble, while **5** is stabilized by 18 kcal/mol due to 6π-electron delocalization, thus explaining the enthalpy difference of 27 kcal/mol between **3** and **5a** ($\Delta_R H(\mathbf{3} - \mathbf{5c}) = 34.8$ kcal/mol, Table 2).

(5) In view of the excess enthalpy of 67.4 kcal/mol and its low kinetic stability (activation enthalpy for ring opening, 4.3 kcal/mol, Table 2), the lifetime of **3** in the gas phase will be very short. The detection of **3** either directly by spectroscopic means or indirectly by bimolecular reactions with suitable scavengers will not be possible. In the solution phase, the lifetime of **3** will be extended, provided that (a) bulky substituents make dissipation of the excess enthalpy possible and (b) the reaction is carried out at low temperature. We suggest that the ozonolysis of bisarylalkynes is carried out at low temperatures in the matrix. Particularly promising should be the ozonolysis of bismesitylacetylene, which should provide the best chance of trapping the corresponding trioxolene.

(6) The peculiarity of the ozonolysis of acetylene (alkynes) results from the fact that the intermediate carbonyl oxide **5** in the form of **5b** can undergo six different reactions with activation enthalpies not larger than 24 kcal/mol (see Scheme 4); i.e., at room temperature and even at lower temperatures, most of these reactions are possible.

Most likely are the isomerization to dioxirane **19** ($\Delta H_a(298) = 16.9$ kcal/mol), the rotation to **5c** ($\Delta H_a(298) = 17.5$ kcal/mol), and the formation of **10** and hydroperoxide **15** ($\Delta H_a(298) = 19.5$ and 20.6 kcal/mol). Less likely is the rearrangement to dioxetanone **9** ($\Delta H_a(298) = 23.6$ kcal/mol). In the absence of alkene, compounds **19**, **10**, **15**, and **9** will rearrange or decompose via relatively small barriers ($\Delta H_a(298) = 12.7$−23.6 kcal/mol, Scheme 4) to anhydride **12**, glyoxal, formaldehyde, formic acid, and (to a minor extent) acid **18**. We note that, in the gas phase, the most likely reaction of radical **16** formed in the OH production step is the abstraction of a H atom from another compound and the formation of **8**, while in solution a reaction in the solvent cage yielding **18** will be possible. We

also note that the reaction possibilities of form **5c** are limited to dioxirane formation, which should increase the yield of anhydride **12** and its decomposition products.

(7) In the presence of alkene, the $[4\pi + 2\pi]$ cycloaddition reaction between **5** and the alkene and the direct epoxidation reaction of the latter by the former have barriers (<3 and 12 kcal/mol)[33] considerably lower than those of any of the six carbonyl oxide reactions shown in Scheme 4. Hence, the most important epoxidation agent in the ozone−acetylene system will be **5**. Trioxolene **3** can, in principle, also act as an epoxidation agent; however, the corresponding barrier is much larger than the barrier to ring opening,[33] which means that **3**, contrary to the expectations of Key and Hamilton, does not play any role in alkene epoxidation reactions. If the temperature is raised, dioxirane **19** will also act as an epoxidation agent. We investigate presently whether **15**, **10**, and **9** can act in this way.[33]

(8) In view of the relatively large stability of carbonyl oxide **5**, there is a good chance of trapping the molecule in an O_2-doped matrix after photochemical decomposition of an α-keto diazo compound, where again the use of mesityl substituents should stabilize the carbonyl oxide and facilitate its detection (reaction 12). A combination of spectroscopic and calculational

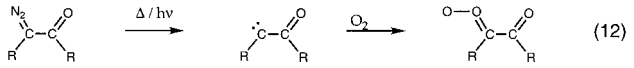

(12)

means would be best for the characterization of 1,2-bismesityl-**5**, as demonstrated in the case of bismesityl carbonyl oxide.[81,82] Tempering of the matrix would make it possible to investigate the unimolecular rearrangement products of the carbonyl oxide.

(9) In this work, we have clarified that the observation of chemiluminescence during the ozonolysis of alkynes[1,8,10,28] results from the decomposition of dioxetanone **9** and/or bicyclic **10**. Previously, **10** was considered to play a role in this connection,[8] but not **9**. In view of an excess enthalpy of at least 63 kcal/mol, **9** will cleave in a symmetry-forbidden reaction to CO_2 and formaldehyde, where the latter molecule will be formed in a triplet excited state, as described in the Discussion part. The triplet state is responsible for the observation of chemiluminescence. It is likely that, in the case of monoalkyl (aryl) acetylenes, the same reaction path can be followed, while in the case of dialkyl (aryl) acetylenes, one has to consider that an alkyl (aryl) group migration would imply a higher barrier for the formation of a dioxetanone.

(10) Similar to the ozonolysis of alkenes, the ozone−acetylene reaction produces OH radicals ($\Delta H_a(298) = 20.6$ and 13.1 kcal/mol) in the gas phase and probably also in solution phase, where in the latter case recombination of OH and radical **16** (Figure 1) in the solvent cage is the most likely reaction. Since acetylene reacts faster with OH radicals than with ozone,[19] OH production by the acetylene ozonolysis is only of relevance for the polluted atmosphere in the absence of OH radicals.

Conclusions 1−10 reveal that the ozonolysis of acetylene possesses one of the most complicated reaction mechanisms investigated; therefore, the reaction deserves intensive experimental studies. A number of experiments are suggested in this work.

Acknowledgment. This work was supported by the Swedish Natural Science Research Council (NFR) and by the Direccin General de Investigacin Cientfica y Tecnica (DGICYT Grant PB98-0278-C02-02). R.C. thanks the CIRIT (Generalitat de Catalunya) for financial support. Calculations were carried out on the supercomputers of the Nationellt Superdatorcentrum (NSC), Linköping, Sweden, and on the IBM SP2 at the CESCA (Barcelona). The authors thank the NSC for a generous allotment of computer time.

Supporting Information Available: Absolute energies, enthalpies, and free energies [Tables A1 (B3LYP results) and A2 (CASSCF, CASPT2 and CCSD(T) results)]; Cartesian coordinates for all structures [Tables A3 (B3LYP results) and A4 (CASCF results)] (PDF). This material is available free of charge via the Internet at http://pubs.acs.org.

JA010166F